END
DATE
FILMED
11 88

MICROCOPY RESOLUTION TEST CHART
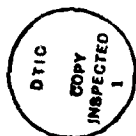NATIONAL BUREAU OF STANDARDS 1963 A

DTIC FILE COPY

④

AD-A199 098

OFFICE OF NAVAL RESEARCH
CONTRACT N0014-85-C-0056
TASK NO. 631-850
TECHNICAL REPORT NO. 17

"Laser Desorption Mass Spectrometry of Substituted Silane High Polymers"

by
T. Magnera, V. Balaji, R. Sooriyakumaran, R.D. Miller, J. Michl

Accession For	
NTIS GRA&I	☒
DTIC TAB	☐
Unannounced	☐
Justification	
By	
Distribution/	
Availability Codes	
Dist	Avail and/or Special
A-1	

DTIC
ELECTE
SEP 0 7 1988
E

Use the title on the front cover.
Per Dr. JoAnn Milliken, ONR/Code 1113

88 8 22 070

REPORT DOCUMENTATION PAGE

1a. REPORT SECURITY CLASSIFICATION	1b. RESTRICTIVE MARKINGS
Unclassified	

2a. SECURITY CLASSIFICATION AUTHORITY	3. DISTRIBUTION / AVAILABILITY OF REPORT
2b. DECLASSIFICATION / DOWNGRADING SCHEDULE	

4. PERFORMING ORGANIZATION REPORT NUMBER(S)	5. MONITORING ORGANIZATION REPORT NUMBER(S)
Technical Report # 17	

6a. NAME OF PERFORMING ORGANIZATION	6b. OFFICE SYMBOL (If applicable)	7a. NAME OF MONITORING ORGANIZATION
IBM Almaden Research Center		ONR

6c. ADDRESS (City, State, and ZIP Code)	7b. ADDRESS (City, State, and ZIP Code)
650 Harry Road San Jose, CA 95120-6099	Office of Naval Research Chemistry Arlington, VA 22217

8a. NAME OF FUNDING / SPONSORING ORGANIZATION	8b. OFFICE SYMBOL (If applicable)	9. PROCUREMENT INSTRUMENT IDENTIFICATION NUMBER
ONR		

8c. ADDRESS (City, State, and ZIP Code)	10. SOURCE OF FUNDING NUMBERS			
	PROGRAM ELEMENT NO	PROJECT NO.	TASK NO.	WORK UNIT ACCESSION NO
Office of Naval Research (Chemistry) 800 Quincy Street Arlington, VA 22217	N0014-85 C-0056		631-850	

11. TITLE (Include Security Classification)

LASER DESORPTION MASS SPECTROMETRY OF ~~POLYSILANES~~ Substituted Silane High Polymers

12. PERSONAL AUTHOR(S) T. Magnera, V. Balaji, R. Sooriyakumaran, R. D. Miller, J. Michl

13a. TYPE OF REPORT	13b. TIME COVERED	14. DATE OF REPORT (Year, Month, Day)	15. PAGE COUNT
Publication	FROM _____ TO _____	8/1/88	69

16. SUPPLEMENTARY NOTATION

Accepted for publication in MACROMOLECULES

17.	COSATI CODES		18. SUBJECT TERMS (Continue on reverse if necessary and identify by block number)
FIELD	GROUP	SUB-GROUP	Polysilane Laser Desorption, Mass Spectrometry, of Fragments, Desorption Mechanism . Silanes,

19. ABSTRACT (Continue on reverse if necessary and identify by block number)

Laser ablation of a variety of polysilanes at 308 nm using fluences of 150-250 mJ/cm² per pulse, well above the photoablation threshold, is a photothermal process and yields products identical to those obtained in vacuum pyrolysis with a CO₂ laser. Unsaturated hydrocarbon products characteristic of the side chains have been identified unequivocally. Silicon-containing products have not been identified individually and it is proposed that they are a mixture of cyclic carbonsilanes, mostly containing no more than two or three silicon atoms linked to each other. A reaction mechanism for the ablation process is proposed and involves no previously unknown reaction steps. The results demonstrate that laser-desorption mass spectrometry will be a good analytical tool for the characterization of this class of polymers. Due to the high volatility of the hydrocarbons, the presence of even quite long side chains on the polymer backbone need not be a source of concern in the applications of the photoablation process.

20. DISTRIBUTION / AVAILABILITY OF ABSTRACT	21. ABSTRACT SECURITY CLASSIFICATION
☐ UNCLASSIFIED/UNLIMITED ☐ SAME AS RPT ☐ DTIC USERS	

22a. NAME OF RESPONSIBLE INDIVIDUAL	22b. TELEPHONE (Include Area Code)	22c. OFFICE SYMBOL

DD FORM 1473, 84 MAR   83 APR edition may be used until exhausted
All other editions are obsolete

LASER DESORPTION MASS SPECTROMETRY OF POLYSILANES

Thomas F. Magnera*, V. Balaji and Josef Michl*

*Center for Structure and Reactivity, Department of Chemistry,
The University of Texas at Austin, Austin, TX 78712-1167*

R. D. Miller and R. Sooriyakumaran,

*IBM Research Laboratories, Almaden Research Center, San Jose, CA
95120-6099*

ABSTRACT

Laser ablation of a variety of polysilanes at 308 nm using
fluences of 150-250 mJ/cm^2 per pulse, well above the
photoablation threshold, is a photothermal process and yields
products identical to those obtained in vacuum pyrolysis with a
CO_2 laser. Unsaturated hydrocarbon products characteristic of
the side chains have been identified unequivocally. Silicon-
containing products have not been identified individually and it
is proposed that they are a mixture of cyclic carbosilanes,
mostly containing no more than two or three silicon atoms linked
to each other. A reaction mechanism for the ablation process is
proposed and involves no previously unknown reaction steps. The
results demonstrate that laser-desorption mass spectrometry will
be a good analytical tool for the characterization of this class
of polymers. Due to the high volatility of the hydrocarbons, the
presence of even quite long side chains on the polymer backbone
need not be a source of concern in the applications of the
photoablation process.

1

INTRODUCTION

High molecular weight polysilanes were probably first prepared over sixty years ago[1] but because of their insoluble and intractable nature elicited little scientific interest. The recent synthesis of soluble derivatives has changed the situation dramatically and led to several proposed applications.[2]

The discovery of rapid ablation of neat solid polysilanes with UV laser light suggested their potential utility as self-developing photoresists.[3] Further interest in this application[4-6] as well as others, such as the use of laser photoablation of polysilanes for optical storage and for their analytical characterization, has prompted the present study. We had two primary objectives:

(i) An assessment of the value of laser desorption mass spectrometry (LDMS), secondary ion mass spectrometry (SIMS), and fast atom bombardment mass spectrometry (FAB) for the structural characterization of polysilanes.

(ii) A probing of the mechanism of polysilane volatilization with 308 nm laser radiation, from the photoablation threshold to higher fluences. The main factor of interest presently is the chemical nature of the ablated materials for a series of polysilane derivatives. The interesting issue of the relative importance of photochemical and photothermal contributions to the process[7-9] will be treated separately.[10]

A brief report of an LDMS investigation of the copolymer of dimethylsilylene and cyclohexylmethylsilylene under conditions of

2

low fluence at shorter wavelengths (248 and 254 nm) has already appeared and a mechanistic scheme for photovolatilization was proposed.[4] We favor a different tentative mechanistic scheme. A preliminary account of our results has appeared in the proceedings of a conference.[11]

The polysilanes we have investigated were the copolymer, poly(dimethylsilane-co-methylcyclohexylsilane) [P-(Me$_2$SiMeChSi)], and the homopolymers poly(dimethylsilane) [P-(Me$_2$Si)], poly(methylcyclohexysilane) [P-(MeChSi)], poly(methylphenyl-silane) [P-(MePhSi)], poly(methyl-n-propylsilane) [P-(MePrSi)], poly(di-n-butylsilane) [P-(Bu$_2$Si)], poly(di-n-pentylsilane) [P-(Pn$_2$Si)], poly(di-n-hexylsilane) [P-(Hx$_2$Si)], and its isotopically labeled variants: fully deuterated on the α carbons (adjacent to Si) [P-(Hx$_2$Si)-α-D], fully deuterated on the β carbons [P-(Hx$_2$Si)-β-D], and fully ^{13}C-labelled on the α carbons [P-(Hx$_2$Si)-α-^{13}C].

The abbreviations introduced in this nomenclature will be used also for smaller fragments. For instance, (Me$_2$Si)$_2$ stands for tetramethyldisilene and Hx$_2$Si for di-n-hexylsilylene.

EXPERIMENTAL PART

Materials. The materials have been synthesized from the appropriate dichlorosilanes by a published procedure[12] except for poly(dimethylsilane), n-hexylsilane and dimethylcyclohexylsilane, which were purchased from Petrarch Systems, Inc. The polysilanes were used in the form of carefully handled thin films or pressed

pellets. Some ambient light exposure was unavoidable but was minimized to avoid photodegradation. The gases used were ultra-high purity and the solvents were reagent grade or better.

Instrumentation (Fig. 1). The experiments were carried out in an ultra-high vacuum chamber equipped with a triple-quadrupole mass spectrometer and various associated components such as a preparation chamber, ion gun etc., described in detail elsewhere.[13] The transmission curve of the mass spectrometer was normalized to the standard spectrum of perfluorotri-n-butylamine. Ionization of ejected matter was either direct (during the ion and atom impact events or during illumination by a pulse of high power focussed UV laser light) or indirect, by electron impact (EI) or multiphoton ionization (MPI) of the neutral ablated material. Mass-analyzed ion intensities were accumulated either in a Nicolet 1170 multichannel analyzer or in a DEC PDP 11/73 computer-based data-collection system.

Collision-Induced Dissociation (CID). Collision-induced dissociation experiments were done as needed on ions for which there was sufficient intensity. All CID spectra were obtained at 5 - 6 eV laboratory collision energy at a collision chamber pressure of 2×10^{-4} torr Ar.

SIMS AND FAB. A 1-μA 4-keV Ar^+ beam was focussed into a 1 mm spot and rastered over a 1 cm^2 target. The resulting ions were pre-filtered in a kinetic energy analyzer and mass analyzed in a quadrupole mass spectrometer. The FAB beam was larger, was not rastered and its intensity was 100 times higher. A low-

. 4

energy electron flood gun was used in both cases to prevent sample surface charging.

LDMS - Electron Impact. A Lumonics HyperEX-400 XeCl excimer laser was used as the source of 308 nm radiation. Approximately 10 percent of the laser output was focussed to a 1×2 mm spot on the polysilane target. This corresponded to a maximum fluence of 250 mJ/cm^2 per pulse at the target after estimating the transmission losses by various optical components between the laser and the target. Standard fluences per pulse were 150-250 mJ/cm^2 at 10 Hz.

When the laser was pulsed at 10 Hz and directed at the target the pressure in the vacuum chamber increased from 10^{-9} torr to between 10^{-7} and 10^{-6} torr. The highest pressure was obtained when irradiating through a freshly cleaned sapphire laser port window. The target was slowly tracked under the focussed spot. Partial overlapping occurs from one pulse to the next, but most of the material exposed is virgin. At the lowest fluences used, 6 mJ/cm^2 per pulse, the frequency had to be increased to about 100 Hz to obtain good spectra and even then, the pressure in the vacuum chamber reached only about 5×10^{-8} torr.

If all the ablated material found its way to the pumps, an average pressure of 5×10^{-7} torr would correspond to a through-put of 10^{-3} torr-l/s which translates to 10^{15} molecules per pulse. This establishes a lower limit of 0.02 molecules ablated per photon. The true ablation rate is much higher since much of

5

the ejected material ends up coating the internal surfaces in the
vacuum chamber. For instance, in ablation rate measurements
using pulses of 308 nm laser light at a fluence of 76 mJ/cm^2 and
a quartz crystal microbalance,[5] the weight loss corresponded to
about 0.16 monomer molecules (SiR$_2$) per photon, or a
corresponding number of molecules of another weight.

Electron impact ionization of the ablated material was done
at two different locations. Fig. 1 indicates the two ionization
regions. The first is just above the surface of the target and
the electron beam is provided by a simple filament floated to -50
V. The second ionization region is provided by the residual gas
analyzer (RGA) filament tucked into the Bessel box kinetic energy
analyzer in front of the first quadrupole. Little or no dif-
ference was detectable in the mass spectra obtained with the two
locations of the filament even though ionization by the RGA
filament required at least one wall collision of the ablated
molecule before it could reach the ionization region.

In order to examine the potential effects of wall collisions
on the ejected neutrals further, time-resolved mass spectra were
measured. After allowing for the ion time of flight, integrated
ion intensity immediately before a pulse was subtracted from the
integrated ion intensity immediately after a laser pulse. The
pre-pulse signal should contain a relatively larger contribution
from molecules that suffered wall collisions than the post-pulse
signal. No appreciable difference in the spectra was noted. In
particular, the generally complicated mass spectra obtained from

6

time-unresolved experiments did not collapse into a simple single parent spectrum. When the RGA filament was the ionization source, it was possible to exclude ions generated directly by laser ionization from the observed spectrum by properly biasing the ion optics. When the ionization region was near the surface, this was not true at high laser powers. A fluence of 250 mJ/cm^2 gave a minimal background.

LDMS - Multiphoton Ionization (MPI). Attempts to use the same 308 nm laser beam for both ablation and direct multiphoton ionization did not give satisfactory results, for two reasons. First, at laser fluences needed for efficient ionization the ablation rate was uncomfortably high. Second, minor variations in laser intensity caused wild fluctuations in signal intensity. Peaks appeared at the same positions in the spectra as in the two-beam experiments described below, but their intensities were nearly random.

Multiphoton ionization mass spectrometry of the ablated material was done for P-(Me_2Si). The excimer beam was divided (9:1) into two beams by a quartz plate. The weaker portion was used for ablation and the remainder was used to pump a Lumonics HyperDYE-300 dye laser. The dye laser beam was focused with a three-element compound lens and directed through a sapphire window to a point approximately 2 mm above the sample surface. The focal point of the dye laser beam was directly above the spot where the ablating 308 nm beam was focused on the target. After passing over the target, the dye laser beam was allowed to strike

7

a Cu foil beamstop attached to the vacuum chamber wall over 10 cm from the target. The dye beam fluence at the beam stop was still sufficiently strong to directly generate Cu ions, which are observed as background in the MPI generated mass spectra. Tight focussing was always required to produce detectable signal levels. At 415 nm a plot of log intensity versus log power had a slope of 1.8, close to the 3/2 power-law saturation limit.[14]

MPI mass spectra obtained at different wavelengths are related to one another through the ion-specific wavelength scan obtained by monitoring the change in the $m/z = 73$ signal as a function of wavelength every 0.5 nm through several overlapping laser dyes at constant energy (15 mJ/pulse). For each dye the working range was limited to that portion for which 15 mJ/pulse output was obtained. The mass spectra were then obtained by data collection and integration over the 2.5 msec post-pulse period for wavelengths 10 nm apart at a constant energy of 15 mJ/pulse.

Trapping of Ablated Neutral Products. Dry N_2 gas was passed rapidly over a polysilane target placed in a quartz cell and focussed 308 nm light was directed at its surface. The stream of N_2 carried the ablated material into a small trap cooled by liquid nitrogen. Rapid streaming was required to keep the walls of the quartz cell clear and to insure that enough material reached the trap. The trap was washed with 10 μl of spectroscopic grade methanol and analyzed in a HP 5995C capillary GC-MS instrument.

Matrix-Isolation Trapping of Ablated Products. The ablation

products were incorporated into a solid argon matrix under vacuum by crossing the ablation plume with a dense (10^{21} molecules/strad) supersonic jet of Ar pulsed at 5-10 Hz, and collecting the resulting gas stream on a cold (20 K) quartz window. The matrix and the material trapped in it were then examined with a Cary-2300 UV-visible spectrometer from 900 to 200 nm. Variation of the laser fluence and of the time lag between the jet nozzle pulse and the laser pulse in a series of experiments permitted a wide variation of the ratio of the ablated material to argon in the matrix. Under no conditions were any absorption bands apparent in the spectra, even in a clear matrix whose subsequent warm-up and evaporation left a visible white residue on the window. The spectra showed only a scattering background, gradually increasing at shorter wavelengths, with an indication of faint shoulders near 250 nm. Optical density reached the value of two near 220 nm.

RESULTS

SIMS-FAB. The salient observed feature is that the spectra of all the polysilane substrates were characterized by the same low-mass ions (m/z = 23, 28, 29, 39, 45, 53, 72). The peaks at m/z = 43, 45, 59 and 73, characteristic of the laser ablation spectra discussed below, were completely absent. The total ion yields were smaller by orders of magnitude compared to the ion yield obtained from a Teflon target under identical conditions. Unlike Teflon, the polysilane samples yielded only negligible amounts of high mass ions. These observations make SIMS

unsuitable for polysilane characterization, in contrast with previously reported results for other polymers.[15] There were no significant differences between spectra generated by fast atoms (FAB) or fast ions (SIMS).

The peaks at m/z = 23, 28, 29, 45 are assigned to Na^+, Si^+, SiH^+, and $SiOH^+$, respectively. The peaks at m/z = 39 are assigned to either NaO^+ or K^+, or both, whereas m/z = 53 and 72 remain unassigned. The ion at m/z = 72 may contain silicon as it underwent CID to produce a weak daughter signal at m/z = 28.

The spectra displayed a slight time dependence. Thus, for P-(Hx_2Si), within the first several minutes a very weak spectrum consisting of numerous peaks separated in groups 14 amu apart was observed. This quickly disappeared in time under the common spectrum reported above and never returned even after hours of continuous sputtering. Reducing the primary beam intensities to move further into the static SIMS regime was not practical due to the already weak signals.

LDMS - EI. The best signal intensities were obtained with laser fluences per pulse between five and six times higher than the 30-50 mJ/cm^2 laser photoablation threshold reported for P-(Pn_2Si),[5] P-(p-t-BuPhMeSi),[5] P-(i-PrMeSi),[6] and P-(PrMeSi).[6] Unless stated otherwise, the spectra shown were obtained with fluences of 150-250 mJ/cm^2 per pulse. The effect of fluence on the relative intensities of MS peaks was investigated for P-(Pn_2Si) and P-($Me_2SiMeChSi$) and was found to be negligible within this range. A detailed examination of P-(Pn_2Si) revealed

10

that the relative intensities of the peaks in the mass spectrum remained constant to fluences down to about 120 mJ/cm^2 per pulse. At lower fluences, the ratio of the intensities of silicon-free ions to the intensities of silicon-containing ions began to decrease (Fig. 2).

Thus, we believe that it is best to separate the discussion of the results obtained in the "normal fluence" range of 150-250 $mJ/cm,^2$ well above the photoablation threshold, from the discussion of the results obtained in the "low fluence" range of 5-10 $mJ/cm,^2$ well below the photoablation threshold, in which certain decomposition processes appear to be suppressed even though some photovolatilization still occurs and the primary polymer chain cracking processes may possibly be the same. The results previously published[4] for $P-(Me_2SiMeChSi)$ using a 248 nm laser and/or a low-pressure mercury lamp were obtained in the "low fluence" mode and fit the pattern observed here in that the reported silicon-free ion intensities were very weak. However, even at the lowest laser fluences used in our work on this copolymer, 5-10 mJ/cm^2 per pulse, we observed these ions more clearly than the previous authors.

NORMAL FLUENCE RESULTS. The electron-impact spectra of the material ablated by focused 308 nm laser light are very complicated (Figures 3-5). Particularly for the polysilanes with small alkyl groups, ions much larger than monomeric $RR'Si^{\bullet+}$ represent the bulk of the ions observed.

The common and/or specific features of the major spectral

11

peaks are:

1. The spectra are dominated by closed-shell (even-electron, odd mass) ions, particularly in the high-mass region. The alkylated polysilanes yield intense Me_3Si^+, Me_2HSi^+, and MeH_2Si^+ peaks. All of the polysilanes except P-(MeChSi) yield significant intensities for the protonated monomers, $RR'HSi^+$. In the P-(Me$_2$SiMeChSi) copolymer the ratio of Me_2HSi^+ to $Me_2Si^{\bullet+}$ is about three, similar to that observed for P-(Me$_2$Si). We were not able to determine the ratio of $MeChHSi^+$ to $MeChSi^{\bullet+}$, due to interference from other peaks. The high-mass region in the spectrum of this 1:1 copolymer is disproportionately dominated by peaks due to the Me_2Si units.

Other alkylated and silylated silicenium cations, including cyclic or unsaturated ones, containing up to five silicon atoms, are abundant in the spectra of the polysilanes with short alkyl chains. Isotopic labelling in P-(Hx$_2$Si) suggests considerable scrambling of hydrogen atoms and of the position of attachment of silicon atoms on the alkyl chain.

2. A few open-shell (odd-electron, even mass) ions are also observed. The radical cation of the monomeric silylene, $R_1R_2Si^{\bullet+}$, is always present but is never significantly stronger than the protonated silylene $R_1R_2HSi^+$, except for P-(MeChSi), where the latter is very weak. If alkyl side chains as long as or longer than propyl are present, a loss of a C_2H_4 unit from the side chain is observed with considerable intensity. Isotopic labeling studies of P-(Hx$_2$Si) showed that at least in this case, the carbon

12

atoms lost are clearly those in the α and β positions in the alkyl group relative to Si.

When R is an n-alkyl group, open-shell ions that correspond to losses from the monomer of alkenes longer than ethylene are also observed. The alkene lost is never longer than R and the ions resulting from these losses decrease in intensity as the length of the alkene shortens. An increase in the loss intensity occurs when the alkene is ethylene.

The radical cation of the disilene, $[RR'Si=SiRR']^{\bullet+}$, is observed with the smaller alkyl groups R and R' and only weakly observed if R and R' are large. The trimeric radical cation $(R_1R_2Si)_3^{\bullet+}$ is weak and is seen only for P-(Me$_2$Si), P-(MePrSi), and in a very low resolution spectrum of P-(Hx$_2$Si).

3. In addition to silicon-containing ions, the mass spectra of all the samples except P-(Me$_2$Si) contain a series of peaks assignable to the MS of one or more hydrocarbons. Their relative intensities are constant but the ratio between the portion of the total spectrum assignable to a hydrocarbon and that assignable to silicon-containing ions is constant only as long as the laser fluence per pulse is well above the ablation threshold (Fig. 2). As the fluence per pulse drops below about 100 mJ/cm,^{2} the ratio drops precipitously and in the low fluence limit it is considerably less than one. Thus, this ratio is the main characteristic that distinguishes normal fluence from low-fluence results.

13

In order to check the possibility that the series of peaks assigned to 1-hexene [from P-(Hx$_2$Si)] and to cyclohexene [from P-(MeChSi)] originate in EI on a silicon-containing precursor which yields C$_6$H$_{12}$$^{\bullet+}$ and C$_6$H$_{10}$$^{\bullet+}$, respectively, that then fragments further, we have compared the relative intensities within each fragmentation series with those obtained from EI on HxSiH$_3$ and ChMe$_2$SiH. These substrates also yield peaks corresponding to C$_6$H$_{12}$$^{\bullet+}$ and C$_6$H$_{10}$$^{\bullet+}$, respectively, but the intensity distribution within each series is quite different from that observed in the LDMS of the polymer substrates. In order to prove conclusively that the MS peaks assigned to hydrocarbons do not originate in the EI event, an attempt was made to trap the hydrocarbons among the neutral ablation products from three of the polymers. In each case, the hydrocarbon was detected unequivocally by low-temperature trapping: 1-hexene from P-(Hx$_2$Si), cyclohexene from P-(MeChSi), and benzene and toluene from P-(MePhSi). The yields were small, presumably due to the inefficiency of the trapping method and not necessarily due to a low absolute yield.

In the following, we describe very briefly the laser-ablation EI mass spectra for each structural group of polysilanes. A detailed description of the results is available in the Supplementary Material.

P-(Me$_2$Si). The ions observed from this substrate (Fig. 3) were the richest in silicon. Most prominent peaks are assigned the structures of closed-shell silicenium cations carrying

14

hydrogen, methyl, and partially or fully methylated silyl substituents: $R_1R_2R_3Si^+$, R=H, Me, Me_3Si, etc. Other closed-shell ions have unsaturated or cyclic structures.

The $Me_2Si^{\bullet+}$ ion is present at about a third of the intensity of Me_2HSi^+. Other important open-shell ions are $Me_2Si=SiMe_2^{\bullet+}$ and an ion at m/z=158, possibly $Me_2Si^{\bullet}-Si(=CH_2)-Si^+Me_2$. The open-shell ion $(Me_6Si_3)^{\bullet+}$ is quite weak and $(Me_8Si_4)^{\bullet+}$ is not observable, but $(Me_{10}Si_5)^{\bullet+}$ appears to be present, albeit weakly. It presumably has a cyclic structure with a five-membered ring of silicons.[16] Several of the assignments were confirmed by CID experiments, and comparison with published data.[17-19]

p-(Hx_2Si) and Its Isotopomers. In a high-sensitivity low-resolution spectrum local relative intensity maxima were found for ions near masses corresponding to $(Hx_2Si)_2^+$, $Hx_3Si_2^+$, Hx_3Si^+, $Hx_2Si^{\bullet+}$ and $HxSi^+$. Peak widths were greater than 5 amu and for example $(Hx_2Si)_2^{\bullet+}$ was therefore not distinguishable from $(Hx_2Si)_2H^+$. Starting with the dimer each local maximum was echoed at masses lower by 28 and 56 amu, corresponding to a loss of one and two molecules of ethylene, respectively.

A series of prominent closed-shell ion peaks (Fig. 4) is most likely associated with singly, doubly, or triply alkylated silicenium cations such as H_2EtSi^+ or HMe_2Si^+ at m/z = 59, through $HEtHxSi^+$ at m/z = 143. The isotopic intensity distributions in the ions $C_3H_9Si^+$ and $C_2H_7Si^+$ in the spectrum of p-(Hx_2Si)-α-^{13}C fit binomial distributions, $[^{13}C_0]:[^{13}C_1]:[^{13}C_2]:[^{13}C_3] = (1-p)^3:3(1-p^2)p:3(1-p)p^2:p^3$, and

15

$[^{13}C_0]:[^{13}C_1]:[^{13}C_2] = (1-p)^2:2(1-p)p:p^2$, with $p = 0.35$. This probability is twice that expected if all carbon positions in the n-hexyl group were equally likely to be bonded to the silicon in the observed ion. If the silicon always stayed attached to its α carbon, the $C_3H_9Si^+$ ion could never contain three ^{13}C atoms. We conclude that the silicon shifts to other carbons extensively, but not randomly.

The more tractable patterns are presented in Fig. 6 which features the quite intense peaks for the HHx_2Si^+ ion at $m/z = 199$ and for the H_2HxSi^+ ion at $m/z = 115$, smaller by C_6H_{12}. α-Substitution by ^{13}C changes the m/z values to 201 and 116, respectively, as expected for the loss of hexene with its α carbon. α-Disubstitution by ^2H changes them to 203 and 117, respectively, indicating that both α-^2H atoms are missing. On the other hand, β-disubstitution by ^2H produces 203 and not only 117 but also an equal amount of 118. Apparently, much of the time, a deuterium atom which was in a β position in the polymer is now located on the Si atom in the hexylsilyl cation. The overall isotopic pattern is compatible with a quite selective cleavage of the Si-C bond and transfer of a β hydrogen on the silicon, resulting in the formation of 1-hexene. It is not clear from the above whether the process occurs before electron impact ionization, or after ionization, or both. However, as we shall see below, CID experiments on analogous ions obtained from P-(Pn_2Si) suggest strongly that at least in that case, the alkene loss from the silicon occurs both before and after ionization.

16

Other series of prominent closed-shell ions correspond to unsaturated, cyclic or bicyclic analogs of the first series.

Intense open-shell ions are assigned to $Hx_2Si^{\bullet+}$, $H_2Hx_2Si^{\bullet+}$, $HHxSi^{\bullet+}$, and $H_3HxSi^{\bullet+}$. Ions associated with formal losses of ethylene, butene (or two molecules of ethylene), pentene, and hexene, respectively, from $Hx_2Si^{\bullet+}$, and with a loss of ethylene from $HHxSi^{\bullet+}$, are also observed.

Isotopic shift patterns are instructive for a few of these ions. The relatively intense open-shell ion peaks at m/z = 170 and m/z = 198 ($Hx_2Si^{\bullet+}$) are related by the loss of C_2H_4 (Figure 6). Upon introduction of α-^{13}C atoms, the peaks shift to m/z = 171 and m/z = 200, showing clearly the loss of one α carbon. Upon dideuteration in either the α or the β position, they shift primarily to m/z = 172 and m/z = 202, but peaks at m/z = 171 and 173 are also significant. These results demonstrate that the ethylene unit missing in the m/z = 170 ion consists of the α and β carbons and their hydrogens, with a moderate amount of scrambling and suggest the $HxBuSi^{\bullet+}$ structure. Once again, we cannot tell whether the α,β ethylene loss occurs before or after electron impact ionization, or both.

The spectrum of P-(Hx_2Si) contains intense peaks at m/z = 84, 69, 56, 55, 42, 41 and 40, in relative abundances that match closely the standard fragmentation pattern of 1-hexene or cyclohexane. Deuteration in the α and β positions leads to molecular ion shifts by +2 and +1, respectively, and introduction of ^{13}C in the α position to a shift by +1, allowing the clear assignment of

17

the spectrum to 1-hexene formed by the cleavage of the Si-C bond and loss of a β hydrogen. There is evidence of a very small amount of scrambling in the labeled positions, and the isotopic behavior is clearly complementary to that described above for closed-shell silicon-containing ions.

It is most economical to assume that the formation of 1-hexene is due to the same loss that has been deduced from the consideration of the closed-shell ions containing silicon (Fig. 6). If this is correct, the β-hydrogen lost from the hexyl chain ultimately ends up on the silicon that carried the hexyl, and the reaction process involved in the ablation can be represented by the partial structures
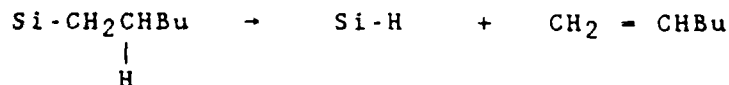
$$Si-CH_2CHBu \quad \rightarrow \quad Si-H \quad + \quad CH_2 = CHBu$$
$$\underset{H}{|}$$

The absence of significant isotopic scrambling in the 1-hexene product suggests that much of the scrambling observed in the closed-shell and open-shell silicon-containing cations results from events not involving the hexyl substituent and quite possibly subsequent to the loss of hexene.

The mass spectra also contain weak unassigned peaks at m/z = 67 and m/z = 70 which may be indications of the presence of cyclohexene and 1-pentene, respectively. Positive identification is prevented by the overlap with the much more intense 1-hexene ion fragmentation pattern.

P-(Pn$_2$Si), P-(Bu$_2$Si) and P-(MePrSi). The silicon-containing

18

ions (Fig. 4) fall in patterns closely similar to those observed for p-(Hx$_2$Si), and peaks due to 1-pentane, 1-butene, and propene, respectively, are intense.

It is significant that CID on the HPn$_2$Si$^+$ ion obtained from p-(Pn$_2$Si) produces a loss of C$_4$H$_8$, presumably to yield HMePnSi$^+$, and a loss of C$_5$H$_{10}$, presumably to yield H$_2$PnSi$^+$, with comparable intensities. Since in the EI mass spectrum of the ablated material, the HMePnSi$^+$ peak is much weaker than the m/z $-$ H$_2$PnSi$^+$ peak, some of the pentene loss apparently occurs already before the ionization event, while some clearly occurs only afterward.

p-(MeChSi). The closed-shell ion series C$_n$H$_{2n+3}$Si$^+$ (Fig. 5) is less prominent than usual and extends only to n $-$ 4. There are considerably fewer closed-shell ions as there is no discernible 14 amu degradation pattern characteristic of the linear alkyls, and only sporadically occurring unsaturated and/or cyclic ions. The protonated monomer peak HMeChSi$^+$ is much weaker than usual, and MeChSi$^{\bullet+}$ is the most intense silicon-containing open-shell ion in the spectrum. The most intense ions in the low-mass portion of the spectrum are due to cyclohexene.

p-(MePhSi). This spectrum (Fig. 5) is very different from the spectra of the alkylpolysilanes. There are very few silicon-containing closed-shell ions, and the normally prominent series C$_n$H$_{2n+3}$Si$^+$ is absent. The observed peaks are assigned to MeSi$^+$, HMePhSi$^+$, Me$_2$PhSi$^+$, and MePh$_2$Si$^+$.

The open-shell ion of the monomer, MePhSi$^{\bullet+}$, is present but

is less intense than the peak due to $PhSi^+$ or an isomer. The low-mass spectrum consisted almost entirely of peaks due to benzene and toluene.

p-(Me₂SiMeChSi). The spectrum of this 1:1 copolymer (Fig. 5) was similar to a superposition of the spectra of p-(Me₂Si) and p-(MeChSi), with the former significantly more intense, particularly in the high mass region where ions containing two or three silicons are much more likely to contain methyl groups than cyclohexyl groups. This may simply be a reflection of the fact that many of the cyclohexyl groups have been lost in the form of cyclohexene. The only open-shell ions with significant intensity are $Me_2Si^{\bullet+}$ ($m/z = 58$) and $Me_2Si=SiMe_2^{\bullet+}$ ($m/z = 116$). The dominant peaks are due to cyclohexene.

LOW FLUENCE RESULTS FOR p-(Me₂SiMeChSi). In order to identify the origin of the large difference between our LDMS of p-(Me₂SiMeChSi) taken at normal fluence (Fig.5) and the spectrum previously reported[4] we have repeated the measurements on this copolymer using laser light fluence reduced to 5-10 mJ/cm^2 per pulse, well below the photoablation threshold reported[5,6] for other polysilanes (30-50 mJ/cm^2). Indeed, the spectrum obtained under these conditions was nearly identical to that previously reported.[4] The remaining differences are probably due to the use of light of a different wavelength and perhaps also to instrumental factors. These are hard to estimate and to eliminate since a detailed description of the previous work[4] has not yet been published.

20

The pattern for closed-shell ions generally resembles that observed for P-(Me$_2$Si) at normal fluence, however relatively more intense ions are observed for H(Me$_2$Si)$_2^+$ (m/z - 117), H(Me$_2$Si)$_3^+$ (m/z - 175) and HMe$_2$SiMe$_2$SiHMeSi$^+$ (m/z - 161). The ion at m/z - 161 is not prominent in the normal-fluence spectrum of P-(Me$_2$Si).

The open-shell ion Me$_2$Si$^{\bullet+}$ (m/z - 58) is relatively less intense than in the spectrum obtained at normal fluences. The ions for (Me$_2$Si)$_2^{\bullet+}$ (m/z - 116) and Me$_2$SiMeChSi$^{\bullet+}$ (m/z - 184) are more intense. We did not observe any significant intensity for MeChSi$^{\bullet+}$ (m/z-126), whereas the published spectrum contains a fair amount.[4]

Much less cyclohexene is generated under the low fluence conditions. As a measure of this the ratio of the silicon-containing ion, Me$_3$Si$^+$ (m/z - 73) to the non-silicon-containing ion, C$_6$H$_{10}^{\bullet+}$ (m/z - 82), changes from 0.25 (normal fluence) to 0.8 (low fluence). Still, the peaks characteristic of cyclohexene were present in our mass spectra under all conditions for which the spectra could be recorded.

LDMS - MPI. An attempt to identify a chromophoric functional group such as silylene in the material volatilized under normal fluence conditions was made using the technique of multiphoton ionization.[14] In order to optimize the chances for survival of the reactive group until the MPI event, we have chosen the polymer with the simplest side group, P-(Me$_2$Si). In this instance, the possible complications due to the otherwise

21

prevalent Si-C bond scission are also absent.

The results of an ion-specific scan from 340 to 520 nm are presented in Figure 7 along with MPI-generated mass spectra at three wavelengths. The distinguishing features in Figure 7 are a broad peak with a maximum between 420 and 430 nm and two small peaks at 460 and 505 nm. In general there are only gradual changes in the MPI mass spectra as a function of wavelength and these can be characterized as an increase in the abundance of the small fragments, $m/z = 43$ and 59, relative to $m/z = 73$, at the two extremes of the scanned region.

MATRIX-ISOLATION TRAPPING. UV-visible examination of the argon matrices containing varying amounts of the ablated material revealed no absorption bands in the 200-900 nm region, and only very weak shoulders near 250 nm.

DISCUSSION

MASS SPECTRA AND STRUCTURE OF THE LASER-ABLATED MATERIAL. *Silicon-containing ions.* Because of the extensive fragmentation and rearrangements in organosilanes after EI ionization,[20] it is not a simple task to assign by EI mass spectrometry alone the structures in what most likely is a mixture of silicon-containing ablated products. A fundamental difficulty is the uncertainty as to how much fragmentation and rearrangement occurs already during the photoablation and how much only after the ionization. Certainly the general features of the spectra, such as high abundance of the Me_3Si^+, Me_2HSi^+, and MeH_2Si^+ peaks and the

22

fragmentation of the alkyl groups in alkylsilicenium ions with loss of ethylene and/or higher alkenes are well known in mass spectrometry of organosilanes.[20]

A consideration of general trends in organosilane mass spectrometry,[20] and a comparison with the information available on EI mass spectra of permethylated short-chain oligosilanes,[19] permethylated small and medium ring cyclosilanes,[16] oligomeric n-hexylsilylenes,[21] oligomeric phenylsilylenes,[21] silenes,[17,22] alkylsilanes,[23] methylphenylsilanes,[23] vinylsilanes,[24] and silacycloalkanes[25] are helpful but permit only limited conclusions.

(i) Organopolysilanes are ablated in a range of sizes from 1 to at least 5 monomer units. The mass spectra are quite reminiscent of those of ordinary saturated acyclic organosilanes, except that they also contain ions poorer in hydrogen, indicating the presence of monocyclic and polycyclic structures, unsaturation, or both. Indeed, similar additional peaks are observed in the spectra of silenes.[17]

(ii) The very low intensity of the higher $(RR'Si)_n^{\bullet+}$ peaks in mass spectra argues strongly against the presence of significant amounts of the isocyclic cyclosilanes $(RR'Si)_n$, known[16] to yield strong parent peaks in EI mass spectra. If cyclic structures are present, they are of the heterocyclic (carbosilane) type. Support for the presence of silacycloalkane or oligosilacycloalkane rings can be seen in the results of isotopic labelling which strongly suggest a migration of silicon to carbon atoms other than α prior to ionization.

23

(iii) From what is known about the decomposition pathways of saturated organooligosilanes,[19] phenylmethylsilanes[23] and oligomeric n-hexylsilylenes,[21] the formation of ions of the type $(R_x R_y Si)_n^+ H$ where R_x and R_y can be Me, Ph or Hx is not common. To account for the prevalence of these ions in our EI mass spectra, structures with SiH bonds must already be present before ionization. Isotopic labeling results suggest that the hydrogens that are transferred to the silicon do not originate only from the α and β positions on the alkyl chain, but to a large degree from the more distant positions.

(iv) We see no particular reason to believe that monomeric silylenes RR'Si: represent the bulk of the ejected neutral fragments, either in the normal-fluence or in the low-fluence regime, particularly when the likely fragmentation of larger molecules after EI ionization is taken into account. To the contrary, unless for some reason they have a very small EI ionization cross section, one can conclude that they can represent at best only a small fraction of the material ablated in the normal fluence regime. This is most obviously apparent in the spectra of the polysilanes with the small R and R' groups, in which ions of larger m/z clearly dominate. No systematic increase in the relative intensity of the RR'Si$^{\bullet+}$ ion compared to other silicon-containing ions is observed as the laser fluence is reduced, and we see no reason to postulate that the silylenes RR'Si: dominate the observed material ejected in the low-fluence regime, as had been proposed earlier,[4] either on the basis of our

24

spectra or of the published[4] spectrum.

It would of course be highly desirable to identify reactive intermediates such as silylenes, silenes, disilenes, silyl radicals, etc., in the observed ablated material since this would provide direct mechanistic information on the chemistry involved in the ablation process. It was with this objective in mind that we performed the MPI-MS and the matrix trapping experiments. The choice of P-(Me_2Si) was dictated by the ready availability of the solution absorption spectra of methyl-substituted organosilicon reaction intermediates and by the limited number of further transformations they might readily undergo, compared with related species containing larger alkyl chains (for instance, chain insertion reactions). Unfortunately, although useful, the evidence provided by the MPI mass spectra and the matrix-isolation trapping spectra is mostly negative: as far as we can tell, there is not only no silylene Me_2Si: in the observed ejected material, as already concluded above, but also no disilene $Me_2Si=SiMe_2$.

The MPI mass spectra of P-(Me_2Si) (Fig. 7) are strikingly similar to the EI spectra and do not change much as the laser wavelength is scanned. At all wavelengths in the region from 340 to 520 nm, they contain significant amounts of peaks larger than $Me_2Si^{\bullet+}$. This is true even in the region near 450 nm, where Me_2Si has its absorption maximum.[26,27] A one-photon resonance should be highly efficient and, if present, already relatively small amounts of Me_2Si: should dominate the spectrum. However, there is

25

only a small peak in the ionization efficiency curve at 450 nm. This cannot be due to a resonance with Me_2Si: absorption, since even at this wavelength, peaks at m/z larger than $Me_2Si^{\bullet+}$ dominate the spectrum.

Along similar lines, $Me_2Si=SiMe_2$ has an absorption maximum near 345 nm[27,28] (tetraalkylsilylenes with bulkier substituents absorb near 390-400 nm[29]) but in this region, we do not observe any dramatic enhancement of the relative intensity of the $Me_4Si_2^{\bullet+}$ ion nor its possible fragments, and ions larger than $Me_4Si_2^{\bullet+}$ represent an important part of the total ion intensity.

The only relatively intense maximum in the ionization efficiency curve occurs between 420 and 430 nm. The absence of discernible maxima in the spectra of matrix-isolated ablated materials makes us believe that neither this, nor the two weak maxima observed at 460 and 505 nm, are due to one-photon resonance enhancement.

Our results do not permit an unequivocal assignment of the origin of the resonances. Possible candidates for two-photon absorption resonances are the trisilane chromophore which absorbs near 215 nm and could be responsible for the strong peak near 420-430 nm in Fig. 7, the linear tetrasilane chromophore which absorbs at 235 nm, and the linear pentasilane chromophore which absorbs near 250 nm.[30] The conspicuous absence of high masses in the spectrum obtained with 505 nm ionizing light and the absence of significant absorption at 250 nm in the matrix-isolation spectrum of the ablated material argue against this last

26

assignment to the pentasilane chromophore, but the location of the trisilane and the tetrasilane absorption peaks is perhaps not a coincidence. An alternative assignment of the 505 nm peak in the ionization efficiency curve would be to a two-photon resonance with the silene chromophore, known to absorb near 260 nm,[27,31] but again, no support for its presence was found in the matrix-isolation spectra. We consider it more likely that the peaks are due to three-photon absorption resonances with chromophores containing fewer than three linked silicons[32] or to resonances in the ionizing transitions rather than the initially absorbing ones. The structures that this suggests for the ablation products are saturated linear or cyclic carbosilanes with no more than two or three silicon atoms linked to each other.

Although the MPI spectra of p-(Me_2Si) do not reveal the actual nature of the ablated material, they are quite unambiguous in excluding the presence of significant amounts of Me_2Si: or $Me_2Si=SiMe_2$. The failure of the matrix-isolation study to detect any absorption bands is compatible with this and moreover suggests that silenes and silyl radicals may well be absent as well. It appears that on a time-scale as short as 1 μs all silicon-centered reactive intermediates are absent in the ablated material; i.e. all initial radiation damage as well as thermal damage has already healed.

Combining the EI and MPI results, we propose that at the time of observation, 1 μs or longer after the 308 nm laser pulse, the ablated material consists primarily of saturated cyclic

27

carbosilanes or C=C unsaturated linear or cyclic carbosilanes with some Si-H bonds and with no more than 2 or 3 Si atoms adjacent to each other.

Silicon-free ions. While the silicon-containing ions in the EI and MPI spectra are definitive in excluding possible constituents and vague in identifying the structures that are actually present in the ablated material, the silicon-free ions are of much direct analytical value. They have not been observed for P-(Me$_2$Si), but in every other case they permit a quite unequivocal identification of a hydrocarbon or hydrocarbons present in the ablated mixture, since the mass spectra of these hydrocarbons are very characteristic. The unlikely possibility that the hydrocarbon parent ion was formed by EI from a silicon-containing material and subsequently underwent the same fragmentation as it normally does when formed by EI on the neutral hydrocarbon was excluded in the case of three of the polymers by the experiment in which the volatile constituents of the ablated material were trapped and subsequently identified by GC-MS.

The hydrocarbons found are terminal alkenes from the alkylated polysilanes, cyclohexene from P-(MeChSi), and benzene and toluene from P-(MePhSi). The formation of very small amounts of methane or ethane from the laser ablation of P-(Me$_2$Si) cannot be excluded. Isotopic labeling on P-(Hx$_2$Si) demonstrated that 1-hexene is formed by scission of an original Si-C bond and removal of one of the β hydrogens.

This previously unobserved hydrocarbon formation provides

28

firmer ground for a mechanistic discussion.

PHOTOCHEMICAL VERSUS PHOTOTHERMAL ABLATION. As discussed in more detail elsewhere,[10] polysilanes provide an interesting test case for weighing the relative importance of the photochemical and photothermal ablation mechanisms, since the nature of the chemical reactions involved in the two processes is different and leaves a clear signature. Since the presently observed C-Si bond scission in a polysilane has never been observed to dominate during irradiation in room-temperature solution,[33] and more important, since it occurs also in the pyrolysis with a low-power CW CO_2 laser,[10] it seems safe to conclude that it is due to a thermal rather than a photochemical process. The virtual identity of the UV laser-desorption and the IR laser-pyrolysis mass spectra of P-(Pn_2Si) suggests that under normal fluence conditions even the former process is predominantly photothermal in nature.[10]
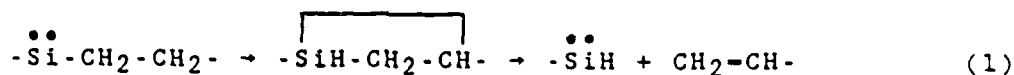
The decrease in the relative intensity of hydrocarbon-derived ions obtained from P-($Me_2SiMeChSi$) when the fluence is reduced below the ablation threshold (Fig. 5) suggests a change in the ablation mechanism at this point. It thus appears likely that in the fast ablation regime, with fluences well above the threshold, the ablation with 308 nm light is primarily photo-thermal while below the threshold it need not be. This might account for the different conclusions concerning the relative importance of the photothermal process reached in ref. 5, which dealt primarily with the regime above this threshold, and in ref. 4, which gives insufficient detail but apparently explored

29

primarily the fluence regime right at or below threshold. Moreover, at the shorter wavelengths used in the latter study the light penetrates deeper, the deposited energy density is lower, and thermal processes may be generally less important.

A TENTATIVE MECHANISM FOR ALKYL POLYSILANE PHOTOABLATION AT 308 NM.

The normal fluence regime. Since we have unambiguously identified only one type of ablation products, we cannot propose a mechanism with a great deal of confidence. However, it is possible to account for all of the observations without postulating any previously undocumented reactions.

To our knowledge, only one class of alkylated silicon compounds has been demonstrated to cleave the Si-C bond readily in a thermal process with the removal of a β hydrogen and formation of a terminal alkene with the same number of carbons. These are the alkylsilylenes[34-37] and the activation energy is about 30 kcal/mol.[38,39] The reaction most likely occurs by silylene insertion into the β C-H bond (1):

$$-\overset{\bullet\bullet}{Si}-CH_2-CH_2- \;\rightarrow\; -SiH-CH_2-CH- \;\rightarrow\; -\overset{\bullet\bullet}{Si}H + CH_2=CH- \qquad (1)$$

A less likely possibility for thermal Si-C bond cleavage is a retro-ene fragmentation of an alkylsilylsilene (2):

$$\qquad (2)$$

30
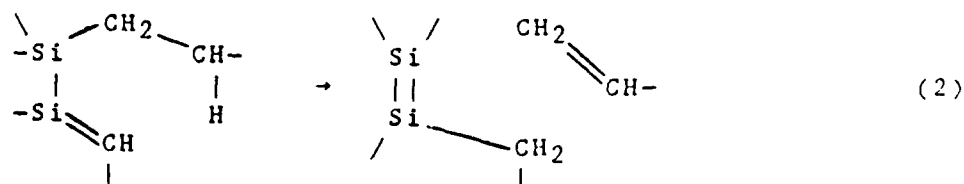
This type of process has never been reported to our knowledge, but there is a report of an analogous retro-ene fragmentation of 1,1-dimethyl-2-neopentylsilene upon its generation by flash vacuum pyrolysis to yield isobutene and dimethylvinylsilane[40] (3):

$$
\begin{array}{c}
CH_3 \quad H{-\!\!-}CH_2 \quad CH_3 \\
\diagdown \qquad\qquad \diagdown \diagup \\
Si \qquad\qquad C \qquad\qquad \rightarrow \\
\diagup \diagdown\diagdown \quad \diagup\diagdown \\
CH_3 \quad CH{-\!\!-}CH_2 \quad CH_3
\end{array}
\quad
\begin{array}{c}
CH_3 \quad H \\
\diagdown \diagup \\
Si \qquad\qquad + \\
\diagup\diagdown \\
CH_3 \quad CH{=}CH_2
\end{array}
\quad
\begin{array}{c}
CH_2 \quad CH_3 \\
\diagdown\diagdown \diagup \\
C \\
| \\
CH_3
\end{array}
\qquad (3)
$$
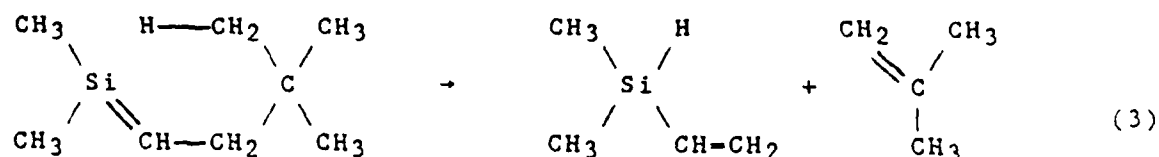
Since the production of two C=C bonds (3) is far more exothermic than the production of one C=C and one Si=Si bond (2) and since we see no evidence of formation of an alkene shorter by two carbons, indicating that (3) is not competitive, we believe that the process (2), although possible in principle, is not competitive either.

An even less likely and undocumented alternative for a thermal Si-C bond cleavage might be a loss of an alkyl radical from the α position in a silyl radical but it appears improbable that the R• radical, if formed, would give rise only to an alkene and no alkane, whose presence would have also been detected in the mass spectrum. The requisite polysilyl radicals should be readily available from the photochemical cleavage of the polysilane chain (4)

$$
SiR_2\text{-}SiR_2\text{-}SiR_2\text{-} \underset{\Delta}{\overset{h\nu}{=}} \text{-}SiR_2\text{-}SiR_2\bullet + \bullet SiR_2\text{-} \qquad (4)
$$
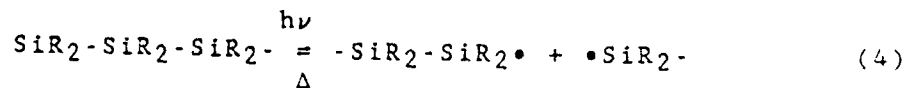
The cleavage (4) might in principle also be induced thermally but would require an activation energy at least equal to the Si-Si

31

bond energy (variously estimated at 80^{41} or 74^{42} kcal/mol; we use the former value throughout in the following for consistency but the arguments are not affected significantly if the lower value is used). Other thermal chain degradation processes would surely occur faster (see below).

Since other reasonable possibilities have not occurred to us, we adopt the process (1) as our working hypothesis for the olefin-producing step. Before accepting the postulate that (1) is the principal alkene-producing reaction, it is important to ask whether it is reasonable to assume that the starting alkylsilylenes can be formed under the reaction conditions. The answer is clearly in the affirmative.

(i) First, there is the hypothetical process (5) proposed in ref. 4 as the main mechanism for polysilane chain degradation:

$$-SiR_2-SiR_2\bullet \rightarrow -SiR_2\bullet + R_2Si: \qquad (5)$$
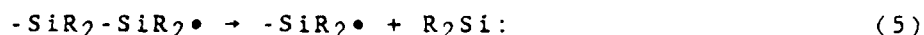
Its activation energy should be slightly in excess of its endothermicity, which can be estimated at 48 kcal/mol (the 80 kcal/mol Si-Si bond energy[41] minus the 32 kcal/mol divalent silicon stabilization energy[43]). The fairly high activation energy is compatible with the observation that at room temperature, $Me_3SiSiMe_2\bullet$ radicals disproportionate and recombine about evenly but do not fragment,[44] and is consistent with the fact that the process (5) has so far never been demonstrated in any system. In fact, one might wonder how it would compete with

32

fragmentation by the more standard β-scission (6):

$$-SiR_2-SiR_2-SiR_2\bullet \rightarrow -SiR_2\bullet + R_2Si=SiR_2 \qquad (6)$$

This, too, has never been proven to occur, but there is evidence
that at high temperatures $Me_3Si-CH_2\bullet$ fragments in a somewhat
analogous fashion to $Me\bullet + Me_2Si=CH_2$,[45] and that $Me_3SiCH_2SiMe_2\bullet$[46]
as well as $Me_3SiSiMe_2CH_2\bullet$[36] fragment to $Me_3Si\bullet$ and $Me_2Si=CMe_2$.
The activation energy of process (6) should exceed slightly its
endothermicity, which can be estimated at ⁻50 kcal/mol (the
difference between the 80 kcal/mol Si-Si bond energy[41] and the
⁻30 kcal/mol energy of the Si=Si π bond[47]). Thus, the
fragmentation (6) might well be competitive with (5).

(ii) A more credible second process available for initial
silylene formation is the well precedented purely thermal
1,1-elimination on silicon (7):

$$-SiR_2-SiR_2-SiR_2-SiR_2- \rightarrow -SiR_2-\overset{\bullet\bullet}{Si}-R + R_3Si-SiR_2- \qquad (7)$$
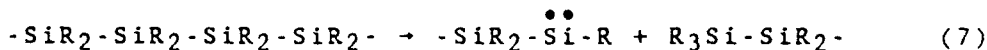
This is known to dominate the pyrolysis of disilanes[41] and
trisilanes[48] and can be quite logically expected to represent the
first step in the pyrolysis of polysilanes as well. Indeed, the
polycarbosilane produced by a 400°C pyrolysis of $P-(Me_2Si)$ is
believed to possess the $(-SiHMe-CH_2-)_n$ unit as the main structural
motif,[2,49] and this is just the structure one would expect from
reaction (7) followed by silylene insertion into the CH bond of a
methyl group.

The endothermicity of reaction (7) can be estimated at

48 kcal/mol, the same as reaction (5). The kinetic parameters of the process $Me_3Si\text{-}SiMe_2H \rightarrow Me_3SiH + Me_2Si:$ are $A - 10^{13}$ s^{-1}, $E_a - 47$ kcal/mol.[41,43] However, unlike (5), process (7) does not require prior photochemical chain scission.

We propose that a combination of steps (7) and (1) is responsible for alkene formation in the IR laser pyrolysis of polysilanes. Moreover, the same combination of steps may be responsible for the formation of alkenes in the UV laser ablation experiments as well: with the above activation parameters, and a reasonable estimate of the hot zone duration (dozens of ns), temperatures of the order 1500-2000 K are required, in perfect agreement with our estimate of about 2000K for the kinetic temperature of the ablated material from the delayed-pulse MPI measurements.[10]

(iii) In the UV laser ablation experiments, another well known way in which a silylene can arise might be operative as well. This third process begins with the homolytic photo-dissociation of an Si-Si bond (4), this time followed by radical disproportionation[2,27,44,50,51] (8) and a subsequent silylsilene to silylmethylsilylene rearrangement[52] (9):

$$-SiR_2\text{-}SiRCH_2R'\bullet + \bullet SiR_2\text{-} \xrightarrow{\Delta} -SiR_2\text{-}SiR{=}CHR' + HSiR_2\text{-} \qquad (8)$$

$$R'HC{=}SiR\text{-}SiR_2\text{-} \xrightarrow{\Delta} -SiR_2\text{-}CHR'\text{-}\overset{\bullet\bullet}{Si}\text{-}R \qquad (9)$$
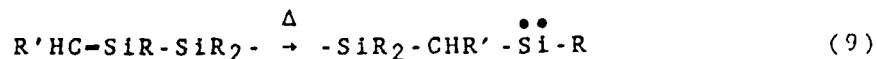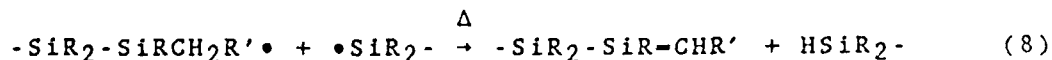
There is some evidence that steps (4) and (8) play a role in solution photochemistry of polysilanes.[33]

34

The hypothesis that the terminal alkene is formed by elimination from alkylsilylene, leaving one of its β hydrogens on the silicon atom, is perfectly compatible with the observed isotopic intensity patterns in both silicon-containing and silicon-free ions. An alternative would be to postulate some other facile but previously undiscovered reaction type. Occam's razor leads us to accept the alkylsilylene hypothesis. Once we do so, the general features of the remainder of the mechanistic picture follow automatically.

In the absence of strain, silylene insertion into a C-H bond has an activation energy of about 20 kcal/mol.[41] This is substantially less than the 30 kcal/mol needed for (1), presumably because of steric strain in the β-insertion transition state. The strain in the silacyclopropane ring has been estimated at ~20[53] or ~23[43] kcal/mol. One would expect less strain in the transition state leading to silacyclobutane, whose ring strain has been estimated at 13 kcal/mol,[53] and very little strain in insertions leading to 5 or 6-membered rings. Even after a consideration of possible differences in the frequency factors, it follows that quite a few ring-forming and possibly some cross-linking C-H insertions must occur if the process (1) occurs, both by silylenes that have not yet eliminated an alkene and those that have. Five-membered and perhaps also six-membered rings should be formed preferentially, but even the insertion that leads to a disilacyclopropane may well be competitive:

35

$$-\overset{\bullet\bullet}{\text{Si}}\text{-CH}_2\text{-CH}_2\text{-CH}_2\text{-R}' \ \rightarrow \ -\text{SiH-CH}_2\text{-CH}_2\text{-CHR}' \qquad (10)$$

$$-\overset{\bullet\bullet}{\text{Si}}\text{-CH}_2\text{-CH}_2\text{-CH}_2\text{-CH}_2\text{R}'' \ \rightarrow \ -\text{SiH-CH}_2\text{-CH}_2\text{-CH}_2\text{-CHR}'' \qquad (11)$$

$$-\overset{\bullet\bullet}{\text{Si}}\text{-SiRCH}_2\text{R}'\text{-SiR}_2\text{-} \ \rightarrow \ -\text{SiH-SiRCHR}'\text{-SiR}_2\text{-} \qquad (12)$$

$$-\overset{\bullet\bullet}{\text{Si}}\text{-[SiRCH}_2\text{CH}_2\text{R}'']\text{-SiR}_2\text{-} \ \rightarrow \ -\text{SiH-[SiRCH}_2\text{-CHR}'']\text{-SiR}_2\text{-} \qquad (13)$$

$$-\overset{\bullet\bullet}{\text{Si}}\text{-[SiRCH}_2\text{-CH}_2\text{-CH}_2\text{R}''']\text{-SiR}_2\text{-} \ \rightarrow \ -\text{SiH-[SiRCH}_2\text{-CH}_2\text{CHR}''']\text{-SiR}_2 \qquad (14)$$

$$-\overset{\bullet\bullet}{\text{Si}}\text{-SiR}_2\text{-SiRCH}_2\text{R}'\text{-SiR}_2\text{-} \ \rightarrow \ -\text{SiH-SiR}_2\text{-SiRCHR}'\text{-SiR}_2\text{-} \qquad (15)$$
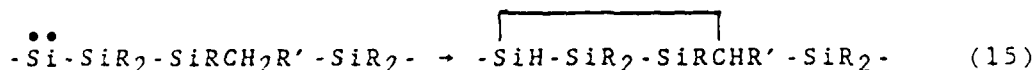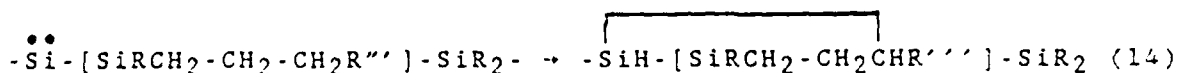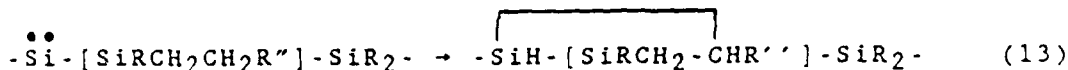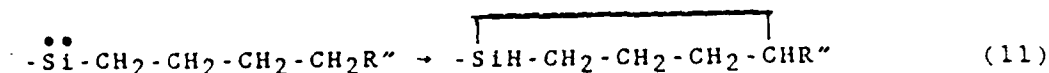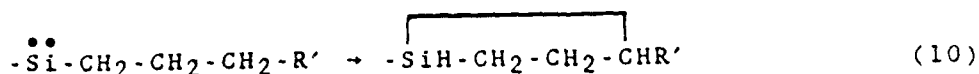
The "healing" of the damage induced by the laser beam should therefore lead rapidly to carbosilane heterocycles containing one or more carbon and one or more silicon atoms, with one or more of the latter carrying a hydrogen. There is precedent for this general type of ring formation in pyrolytic processes involving silylsilylene intermediates.[27,48,54]

A second thermal or photochemical chain rupture, possibly nearly concurrent with the first one, is required to produce a low molecular weight fragment, unless the initial scission happened near a chain end. The second damage site could again repair in an analogous fashion, ultimately producing a bicyclic heterocycle.

Other well-established facile thermal reactions of silylalkylsilylenes are their reversible rearrangement to disilenes and silenes by a hydrogen shift, albeit with somewhat

36

higher activation energies (~ 40 kcal/mol for the latter[55,56]).
Silylene-to-silylene rearrangements are also well documented and
will make it difficult to assess the relative importance of
processes (8) + (9) versus (7). Thus, the insertion step (12)
can be followed by extrusion steps such as (16):

$$-\overset{\boxed{}}{\text{SiH-SiRCHR}'}-\text{SiR}_2- \rightarrow -\overset{\bullet\bullet}{\text{Si}}-\text{CHR}'-\text{SiHR-SiR}_2- \qquad (16)$$
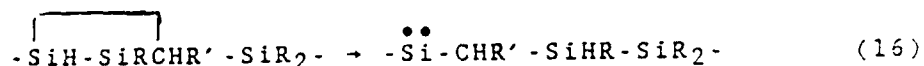
This type of thermal chemistry is well known from the tetra-
methyldisilene-to-1,3-disilacyclobutane rearrangement.[27,53,57]
Alternatively, a silyl shift[52] in an intermediate silylsilene can
also accomplish the interconversion:

$$-\text{SiR}_2-\overset{\bullet\bullet}{\text{Si}}-\text{CH}_2\text{R}' \rightarrow -\text{SiR}_2-\text{SiH=CHR}' \rightarrow \text{H}-\overset{\bullet\bullet}{\text{Si}}-\text{CHR}'-\text{SiR}_2- \qquad (17)$$
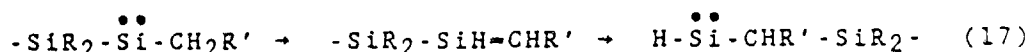
Similar silyl shifts in silyldisilenes are very facile and
should permit a ready isomerization of the initially formed
silylene to another. Thus, the first step of the sequence (18) is
fast already at room temperature[58] and the calculated activation
energy is only 8 kcal/mol:[59]

$$\overset{\bullet\bullet}{\text{HSi}}-\text{SiR}_2-\text{SiR}_2- \rightarrow -\text{SiR}_2-\text{HSi=SiR}_2 \rightarrow -\text{SiR}_2-\overset{\bullet\bullet}{\text{Si}}-\text{SiHR}_2 \qquad (18)$$

The disilene is not likely to accumulate, since the reverse silyl
shift is calculated to have an activation energy of only 17
kcal/mol[59] and the hydrogen shift shown in (18) will also be very
facile. Thus, although processes such as (16)-(18) permit
considerable variation in the structure of the silylene moiety,
the final thermodynamic sinks are still likely to be the products

37

of a C-H or Si-H insertion reaction by a silylene.

It would be useless at the present time to speculate which of the various paths will be most important. However, the observed mass spectra of alkylated polysilanes are clearly compatible with the conclusion that we believe follows automatically once reaction (1) is accepted as the alkene-forming process: in addition to the alkene, the ablated material then must consist primarily of alkylated polysilacycloalkanes and polysilabicycloalkanes, with some Si-H bonds, and possibly with some unsaturation. Note in particular that ring-forming silylene insertions provide a natural explanation for the migration of hydrogen atoms from α, β, and even more so, from more distant positions of the alkyl chain onto silicon. At the same time, it accounts for the transfer of the Si atoms to carbon atoms other than α.

The situation is less clear in the case of aryl substituted polysilanes. It is possible that the benzene observed in photoablation of r-(MePhSi) originates in a homolyric cleavage of a Si-C_6H_5 bond followed by hydrogen abstraction, and that the toluene originates in a 1,1-elimination on silicon at some stage in the decomposition process. Much additional work and isotopic labeling experiments are needed before a credible mechanistic postulate can be formulated.

Low-fluence regime. The primary change in the observed LD mass spectrum of r-(Me$_2$SiMeChSi) that occurs upon reduction of the fluence per pulse below the threshold value is the decrease

38

of the relative abundance of the ions due to cyclohexene. The most economical way of accounting for this change is to postulate that alkylated silylenes still occur as intermediates below the threshold fluence but the lower temperature of the irradiated region no longer suffices for reaction (1) to proceed efficiently (possibility A). An alternative is to postulate that no alkyl-silylenes are present since at the lower temperatures (7) has been shut down and a purely photochemical degradation proceeds by some totally different path that avoids all alkyl-bearing silylenes altogether (possibility B).

We consider possibility A first. In this case, if the process (1), with activation energy of 30 kcal/mol, is nearly shut down, it is reasonable to assume that thermal radical fragmentation processes of higher activation energy, such as (5) or (6), are shut down as well, even though we have no reliable knowledge of their frequency factors. The thermal chain degradation process (7) can then also no longer operate. On the other hand, the photochemical bond cleavage (4), the extremely facile process (8), and even the isomerization processes such as (9) and (18) and silylene insertion reactions such as (10) - (15), characterized by lower activation energies, might well still be going on. Then, the final ablation products would be very similar in structure to those resulting in the normal fluence regime, except that the silicon atoms would still carry their alkyl groups and silylene insertion reactions and silyl radical disproportion-ation would be the only source of Si-H bonds. Considering that ou

39

CID experiments demonstrated that the alkyls can also easily be lost from silicon after electron-impact ionization, this is nicely compatible with the general similarity between the silicon-containing ion parts of the LD mass spectra observed at normal and at low fluence.

Possibility B requires that the similarity of the EI mass spectral patterns for the silicon-containing ions between the normal-fluence and the low-fluence regime be coincidental. Either a separate photochemical path that does not involve ablated silylenes accidentally produces the same chemical structures in the ablated material as the normal-fluence photothermal path, or another set of chemical structures produced in the photochemical path accidentally yields the same mass spectrum. While this possibility cannot be excluded at present, we consider it unlikely.

We do not view the mechanism previously proposed[4] for low-fluence 248 nm photoablation of $P-(Me_2SiMeChSi)$, consisting of steps (4), (5), and hydrogen abstraction by silyl radicals with formation of carbon-based radicals, to be a viable candidate for the low-fluence 308 nm ablation investigated here. It is not particularly convincing even for the 254 nm photovolatilization. Unlike the authors of ref. 4, we see few, if any, indications in the published[4] mass spectra that the silylenes Me_2Si: and $MeChSi$: represent the bulk of the observed ablated material (nor is such evidence present in our mass spectra, obtained at the 308 nm ablation wavelength). It is hard to see how a thermal chain

40

degradation process (5) with an activation energy of at least 48 kcal/mol could be responsible for the accumulation of any significant amount of MeChSi:, given that the activation energy for the fragmentation of the latter to MeHSi: and cyclohexene cannot be very different from 30 kcal/mol. Yet, no cyclohexene was observed in the mass spectra of ref. 4 (and little is observed in our low-fluence spectra). Also, the process (6) is likely to be reasonably competitive with (5) but there is no indication that it is taking place. Finally, the abstraction of hydrogen atoms from unactivated C-H bonds in an alkyl chain by silyl radicals with formation of carbon-based radicals is endothermic and processes such as (8) and (10) - (15) are far more likely sources of Si-H bonds.

IMPLICATIONS FOR THE ANALYSIS OF POLYSILANES. Surface contamination and/or light-induced surface photochemistry in the presence of O_2 is most likely responsible for the lack of substrate specificity in SIMS and FAB. Means to avoid this type of problem would inevitably be cumbersome. These observations make these two methods unsuitable as analytical tools for solid polysilanes.

On the other hand, the very characteristic side chain losse: in LDMS, particularly at the higher laser fluences, make this an excellent method for polysilane characterization. It actually appears likely that the simpler and cheaper procedure of laser desorption gas chromatography or even ordinary pyrolysis gas chromatography would work well.

41

IMPLICATIONS FOR THE USE OF POLYSILANES AS SELF-DEVELOPING PHOTORESISTS. The observation of an extensive thermal loss of the side chains in the photoablation process in the form of hydrocarbons has an important consequence for possible practical uses. Since the hydrocarbons are volatile, the presence of even quite long side chains on the polymer backbone need not be a source of concern. Such polymers may offer easier processing and other advantages. In order to increase the volatility of the silicon-containing products, it would be helpful to build silylene-scavenging groups into the side chains or to make them otherwise available, thus suppressing the cyclizing and cross-linking processes due to the postulated insertion of silylenes into CH bonds. Atmospheric oxygen is one possible choice[4] but is not ideal since it produces silanones which oligomerize, yielding materials of limited volatility.

In order to proceed further, it would be desirable to produce larger amounts of the silicon-containing ablation products, to separate the individual components, and to characterize their individual structures. Since the identity of the products obtained by 308 nm laser ablation and by simple heating has now been demonstrated, this has become a much simpler task. The investigation of the mechanism of polysilane laser photoablation has thus been closely linked to investigations of its thermal conversion to silicon carbide.[49]

42

Supplementary Material Available. A description of the laser-desorption electron-impact mass spectra of polysilanes, 13 pages. Ordering information is given on any masthead page.

REFERENCES

1. Kipping, F. S. J. Chem. Soc. 1924, 125, 2291.

2. West, R. J. Organomet. Chem. 1986, 300, 327.

3. Hofer, D. C.; Jain, K.; Miller, R. D. IBM Tech. Discl. Bull.
   1984, 26, 5683.

4. Zeigler, J. M.; Harrah, L. A.; Johnson, A. W. Proc. of SPIE,
   Advances in Resist Technology and Processing II, 1985, 539,
   166.

5. Marinero, E. E.; Miller, R. D. Appl. Phys. Lett., 1987, 50,
   1041.

6. Hansen, S.G.; Robitaille, T.E. J. Appl. Phys. 1987, 62,
   1394.

7. Srinivasan, R.; Mayne-Banton, V. Appl. Phys. Lett. 1982, 41,
   576; Srinivasan, R., Leigh, W. J. J. Am. Chem. Soc. 1982,
   104, 6784.

8. Srinivasan, R. Science (Washington, D.C.) 1986, 234, 559.

9. Srinivasan, R.; Braren, B.; Dreyfus, R.W. J. Appl. Phys.
   1987, 61, 372; Gorodetsky, G.; Kazyaka, T. G.; Melcher,
   R.L.; Srinivasan, R. Appl. Phys. Lett. 1985, 46, 828;
   Brannon, J.H.; Lankard, J.R.; Baise, A.I.; Burns, F.;
   Kaufman, J. J. Appl. Phys. 1985, 58, 2036.

10. Magnera, T.F., Balaji, V.; Michl, J.; Miller, R.D.,
    manuscript in preparation.

11. Magnera, T.F.; Balaji, V.; Michl, J.; Miller, R.D., Proceed-
    ings of the 8th International Symposium on Organosilicon
    Chemistry, Ellis Horwood, Ltd., Chichester, in press.

12. Miller, R. D.; Hofer, D.; McKean, D. R.; Willson, C. G.;
     West, R.; Trefonas, P. III in "Materials for Microlithog-
     raphy", ACS Symposium Series No. 266, Thompson, L. F.;
     Willson, C. G.; Frechet, T. M. J. eds., American Chemical
     Society, Washington, D.C., 1984, p. 293.

13. Magnera, T. F.; David, D. E.; Orth R.; Stulik, D.; Jonkman,
     H. T.; Michl, J., submitted for publication.

14. Lin, S.H.; Fujimura, Y.; Neusser, H. J.; Schlag, E. W.
     "Multiphoton Spectroscopy of Molecules", Academic Press
     Inc., New York 1984.

15. Werner, H. W. Mikrochim. Acta Suppl. VII, 1977, 63; Müller,
     G. Appl. Phys. 1976, 10, 317; Gardella, Jr., J. A.;
     Hercules, D. M. Anal. Chem. 1980, 52, 226; Briggs, D. Surf.
     Interface Anal. 1983, 5, 113; K. Okuno, S. Tomita and A.
     Ishitani, "Secondary Ion Mass Spectrometry SIMS IV" Ed. A.
     Benninghoven, J. Okano, R. Shimizu and H. W. Werner,
     Springer-Verlag, Berlin, 1984, p. 392.

16. Kinstle, T. H.; Haiduc, I., Gilman, H. Inorg. Chim. Acta
     1969, 3, 373.

17. Pope, K. R.; Jones, P. R. Organometallics 1984, 3, 354.

18. Groenewold, G. S.; Gross, M. L.; Bursey, M. M.; Jones, D. R.
     J. Organomet. Chem. 1982, 235, 165.

19. Nakadaira, Y.; Kobayashi, Y.; Sakurai, H. J. Organomet.
     Chem. 1973, 63, 79;

20. Schwarz, H., in "The Chemistry of Organosilicon Compounds",
     Patai, S.; Rappoport, Z., eds., Wiley, New York, in press.

21. Aitken, C.; Harrod, J. F.; Gill, U. S. <u>Can. J. Chem.</u>, 1987, <u>65</u>, 1804.

22. Brook, A. G.; Harrison, A. G.; Kallury, R. K. M. R. <u>Org. Mass Spectrom.</u> 1982, <u>17</u>, 360.

23. Gaidis, J. M.; Briggs, P. R.; Shannon, T. W. <u>J. Phys. Chem.</u> 1971, <u>75</u> 974; Chernyak, N.Ya.; Khmel'nitskii; D'yakova, T.V.; Vdovin, V.M. <u>Zh. Obshch. Khim.</u> 1966, <u>36</u>, 89.

24. Polivanov, A. N.; Bernadskii, A. A.; Zhun, V. I.; Bochkarev, V. N. <u>Zh. Obshch. Khim.</u> 1978, <u>48</u>, 2703.

25. Chernyak, N.Ya.; Khmel'nitskii, R.A.; D'yakova, T.V.; Vdovin, V.M.; Arkhipova, T.N. <u>Zh. Obshch. Khim.</u> 1966, <u>36</u>, 96.

26. Drahnak, T. J.; Michl, J.; West, R. <u>J. Am. Chem. Soc.</u> 1979, <u>101</u>, 5427.

27. Raabe, G.; Michl, J. <u>Chem. Rev.</u> 1985, <u>85</u>, 419.

28. West, R.; Fink, M.J.; Michl, J. <u>Science (Washington, D.C.)</u> 1981, <u>214</u>, 1343.

29. Watanabe, H.; Kougo, Y.; Kato, M.; Kuwabara, H.; Okawa, T.; Nagai, Y. <u>Bull. Chem. Soc. Japan</u> 1984, <u>57</u>, 3019.

30. R. West, in "Comprehensive Organometallic Chemistry", Wilkinson, G.; Stone, F. G. A.; Abel, E. W. eds., Pergamon Press, Oxford, 1982, Vol. 2, 365.

31. Drahnak, T. J.; Michl, J.; West, R. <u>J. Am. Chem. Soc.</u> 1981, <u>103</u>, 1845.

32. Already a single saturated carbon effectively separates two silicon-based chromophores; Pitt, C. G.; Habercom, M. S.;

46

Bursey, M. M.; Rogerson, P. F. J. Organomet. Chem. 1968, 15, 359.

33. For a brief recent review of the solution photochemistry of polysilanes see Michl, J.; Downing, J. W.; Karatsu, T.; Klingensmith, K. A.; Wallraff, G. M.; and Miller, R. D., in "Inorganic and Organometallic Polymers," ACS Symposium Series, Zeldin, M.; Wynne, K. eds., American Chemical Society, Washington, D.C., in press. In work to be published, we have found that reductive elimination on silicon with C-Si bond scission does represent a minor path in the solution photolysis of $P-(Hx_2Si)$. We have searched for hexane among the products and found none with a detection limit of 0.03% of the hexyl groups present. If hexene were formed in the experiment, it would remain undetected, since it does not survive the reaction conditions, as has been verified in a control experiment.

34. Barton, T. J.; Burns, G. T. Organometallics 1983, 2, 1.

35. Gusel'nikov, L. E.; Lopatnikova, E.; Polyakov, Yu. P.; Nametkin, N. S. Dokl. Akad. Nauk, USSR 1980, 253, 1387.

36. Gusel'nikov, L. E.; Polyakov, Yu. P.; Volnina, E. A.; Nametkin, N. S. J. Organomet. Chem. 1985, 292, 189.

37. Barton, T. J.; Tillman, N. J. Am. Chem. Soc. 1987, 109, 6711.

38. Rickborn, S. F.; Ring, M. A.; O'Neal, H. E. Int. J. Chem. Kinetics 1984, 16, 1371.

39. Sawrey, B. A.; O'Neal, H. E.; Ring, M. A.; Coffey, D., Jr. Int. J. Chem. Kinetics 1984, 16, 801.

40. Conlin, R. T.; Bessellieu, M. P.; Jones, P. R., Pierce, R. A. Organometallics 1982, 1, 396.

41. Davidson, I. M. T.; Howard, A. V. J. Chem. Soc. Faraday Trans. 1 1975, 71, 69; Davidson, I. M. T.; Matthews, J. I. J. Chem. Soc. Faraday Trans. 1 1976, 72, 1403.

42. Walsh, R. Acc. Chem. Res. 1981, 14, 246.

43. Walsh, R. J. Phys. Chem. 1986, 90, 389.

44. Hawari, J. A.; Griller, D.; Weber, W. P.; Gaspar, P. P. J. Organomet. Chem. 1987, 326, 335..

45. Potzinger, P.; Reimann, B.; Roy, R. S. Ber. Bunsenges. Phys. Chem. 1981, 85, 1119.

46. Davidson, I. M. T.; Potzinger, P.; Reimann, B. Ber. Bunsenges. Phys. Chem. 1982, 86, 13.

47. Michalczyk, M. J.; West, R.; Michl, J. Organometallics 1985, 4, 826.

48. Chen, Y. S.; Cohen, B. H.; Gaspar, P. P. J. Organomet. Chem. 1980, 195, C1.

49. Yajima, S.; Okamura, K.; Hayashi, J. Chem. Lett. 1975, 1209.

50. Gammie, L.; Safarik, I.; Strausz, O. P.; Roberge, R.; Sandorfy, C. J. Am. Chem. Soc. 1980, 102, 378.

51. Cornett, B. J.; Choo, K. Y.; Gaspar, P. P. J. Am. Chem. Soc. 1980, 102, 377; Doyle, D. J.; Tokach, S. K.; Gordon, M. S.; Koob, R. D. J. Phys. Chem. 1982, 86, 3626.

52. Barton, T. J.; Burns, S. A.; Burns, G. T. Organometallics 1982, 1, 210.

53. Davidson, I. M. T.; Scampton, R. J. J. Organomet. Chem. 1984,

<u>271</u>, 249.

54. Davidson, I. M. T.; Hughes, K. J.; Scampton, R. J. <u>J. Or-ganomet. Chem.</u> 1984, <u>272</u>, 11.

55. Schaefer III, H. F. <u>Acc. Chem. Res.</u> 1982, <u>15</u>, 283; Nakase, S.; Kudo, T. <u>J. Chem., Soc. Chem. Commun.</u> 1984, 141.

56. Davidson, I. M. T.; Ijadi-Maghsoodi, S.; Barton, T. J.; Tillman, N. <u>J. Chem. Soc., Chem. Commun.</u> 1984, 478.

57. Conlin, R. T.; Gaspar, P. P. <u>J. Am. Chem. Soc.</u> 1976, <u>98</u>, 868.

58. Sakurai, H.; Nakadaira, Y.; Sakaba, H. <u>Organometallics</u> 1983, <u>2</u>, 1484.

59. Nagase, S.; Kudo, T. <u>Organometallics</u>, 1984, <u>3</u>, 1320.

Captions to Figures

Figure 1. Laser desorption mass spectrometer. (A), (B): Alternative locations of the ionizing filament; T : Movable target; B : Bessel-box energy filter; MS1, MS2: quadrupole mass filters; C : collision cell; D : ion detector; L : laser light beam.

Figure 2. Ratio of the $C_5H_{10}^{\bullet+}$ and Me_3Si^+ ion intensities in the laser desorption electron impact mass spectrum of P-(Pn$_2$Si) as a function of laser fluence per pulse.

Figure 3. Low-resolution (a) and high-resolution (b) laser desorption electron impact mass spectrum of P-(Me$_2$Si).

Figure 4. Laser desorption electron impact mass spectrum of (a) P-(MePrSi), (b) P-(Bu$_2$Si), (c) P-(Pn$_2$Si) and (d) P-(Hx$_2$Si) targets.

Figure 5. Laser desorption electron impact mass spectrum of (a) P-(MePhSi), (b) P-(MeChSi) and (c) P-(Me$_2$SiMeChSi) targets at normal laser fluence and (d) P-(Me$_2$SiMeChSi) at low laser fluence.

Figure 6. Representative isotope patterns in the laser desorption electron impact mass spectra of isotopically labeled P-(Hx$_2$Si).

Figure 7. Laser desorption multiphoton ionization mass spectrum of P-(Me$_2$Si) at (a) $\lambda = 435$ nm, (b) 465 nm, and (c) 505 nm (bottom) and the wavelength dependence of the abundance of the Me_3Si^+ peak (top).
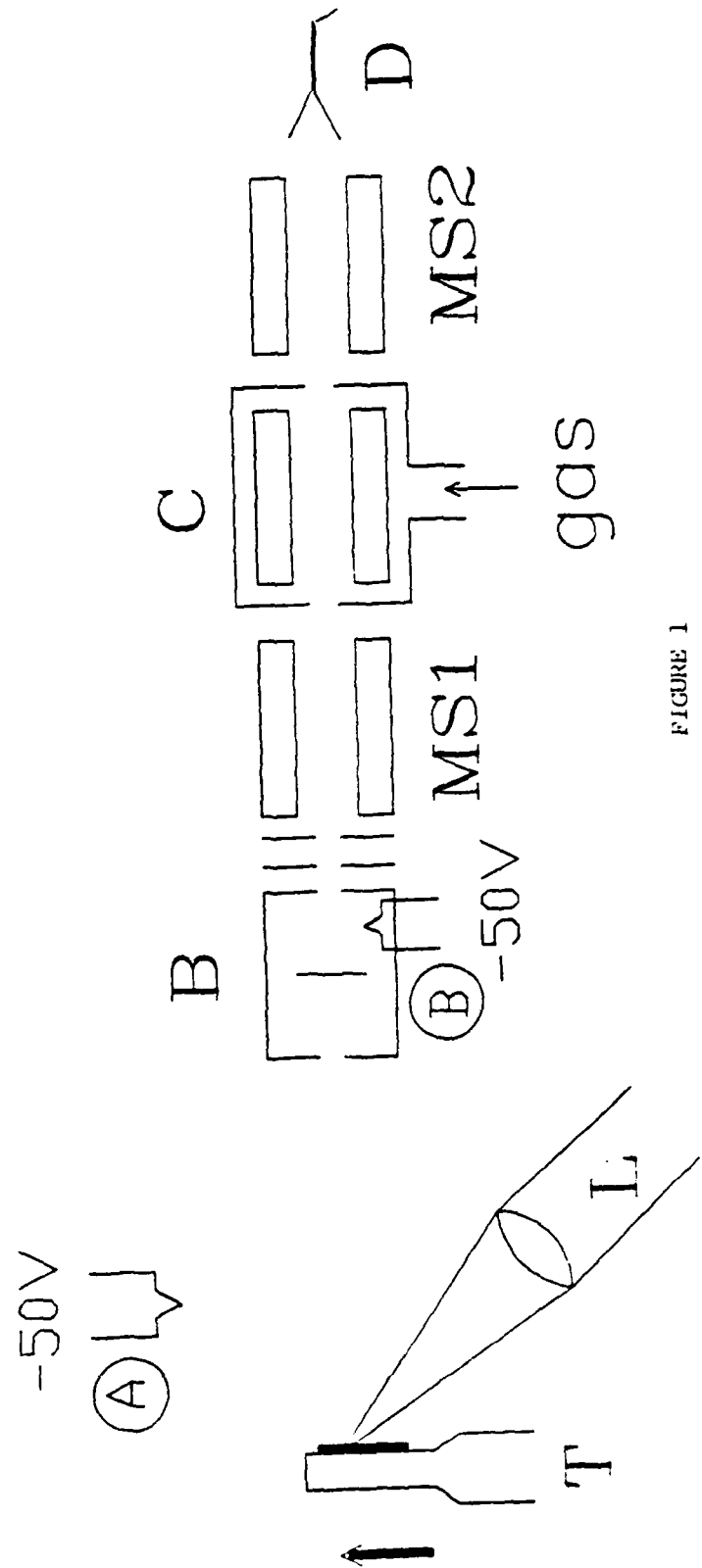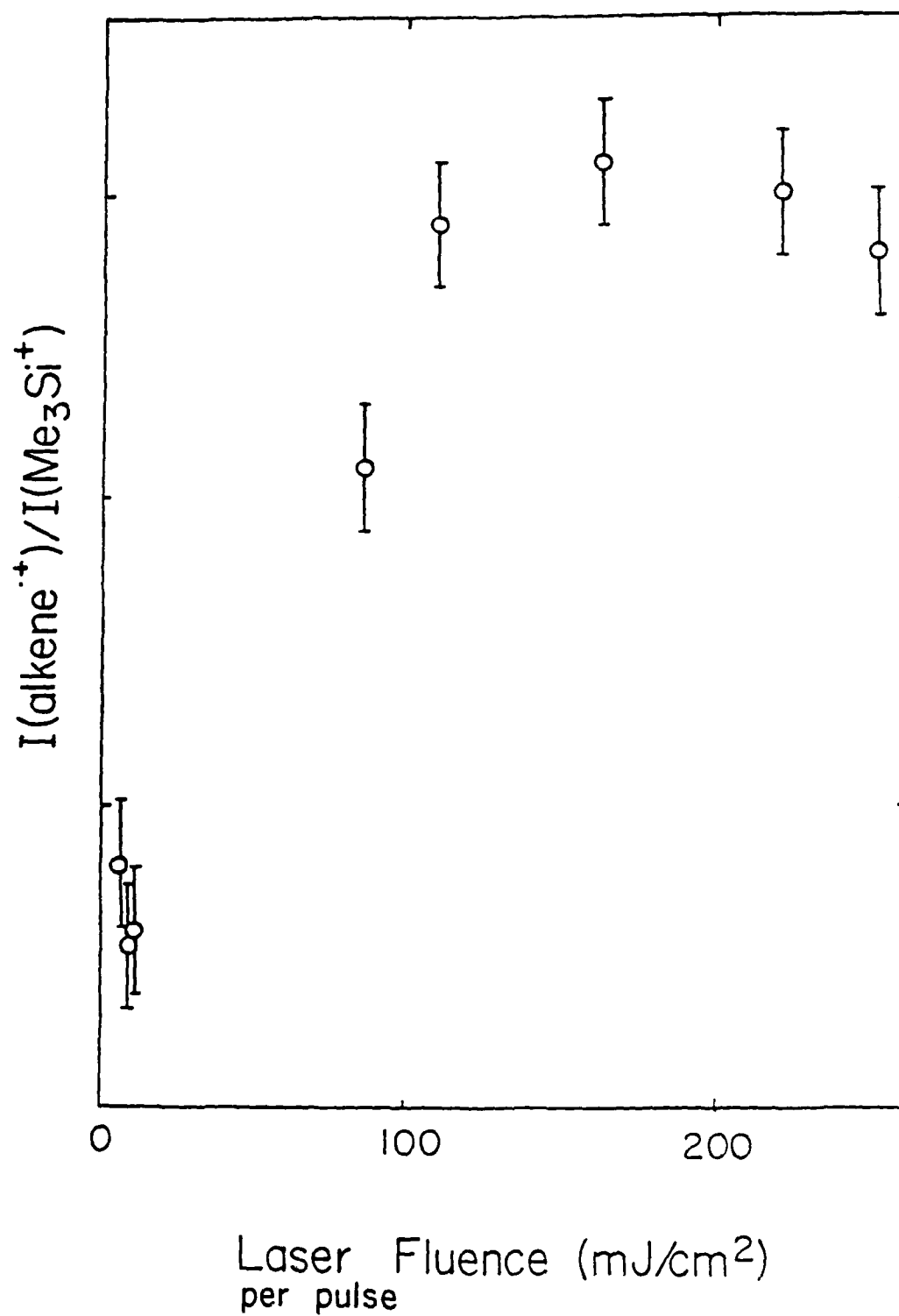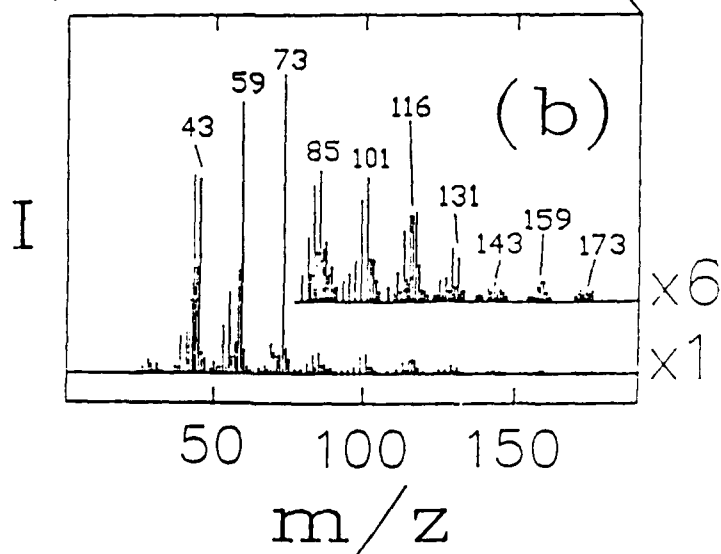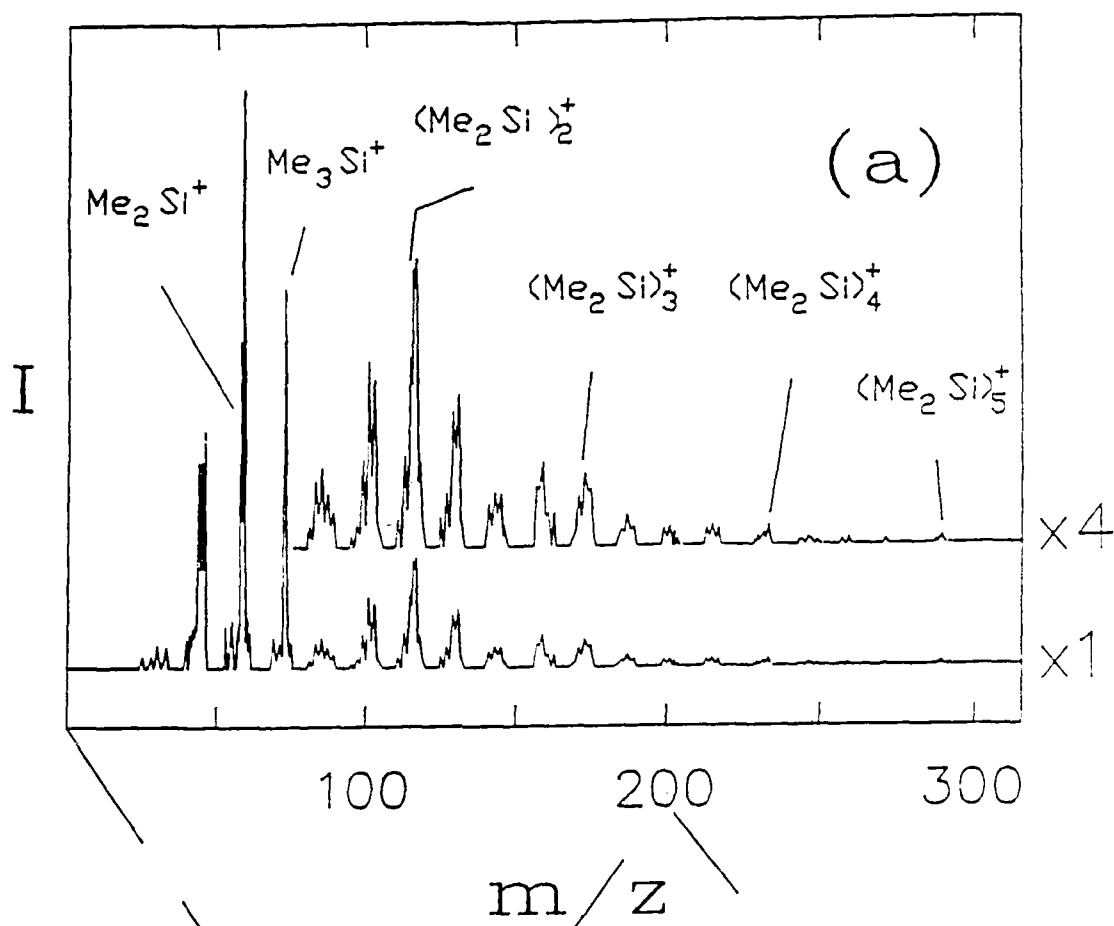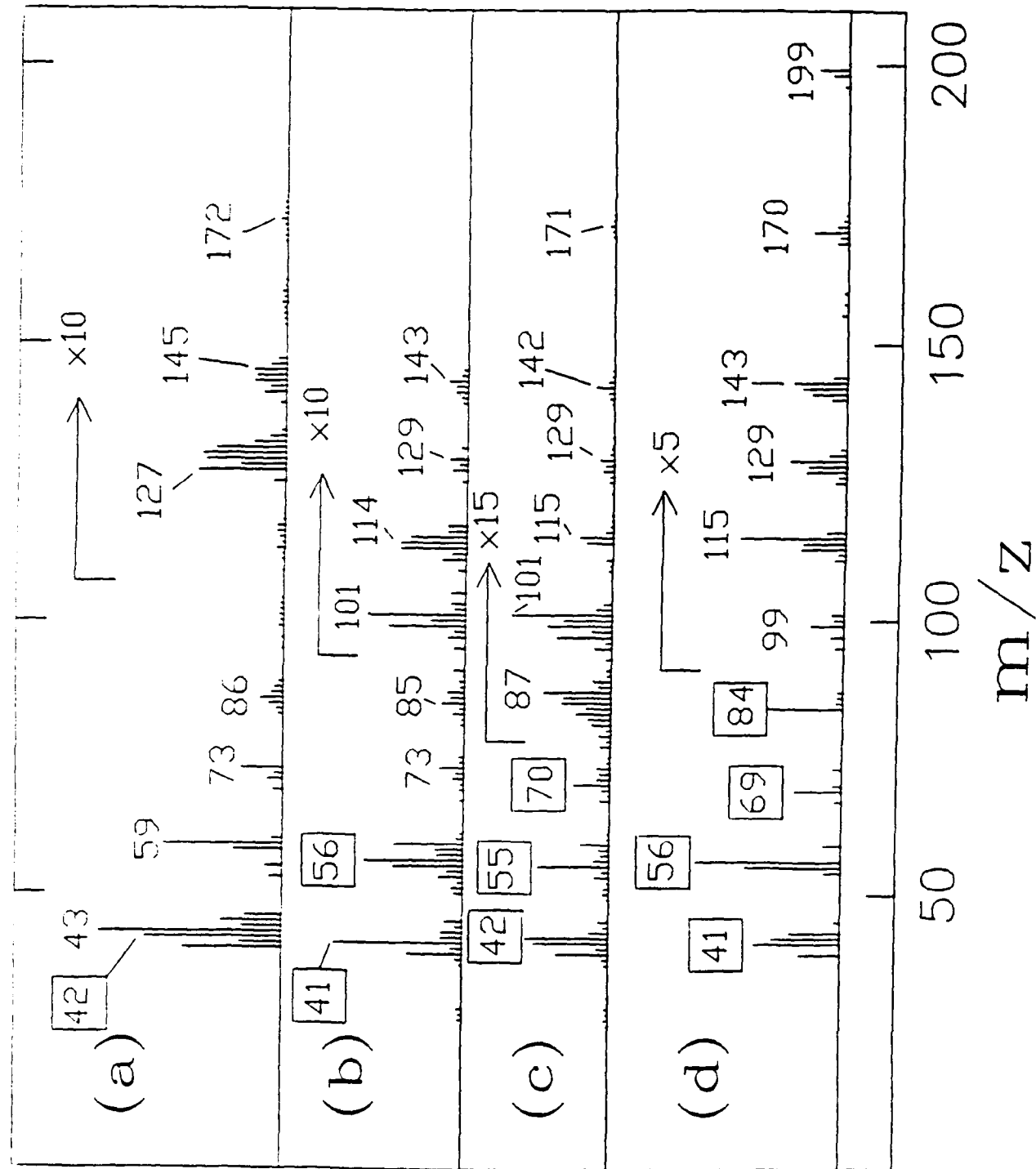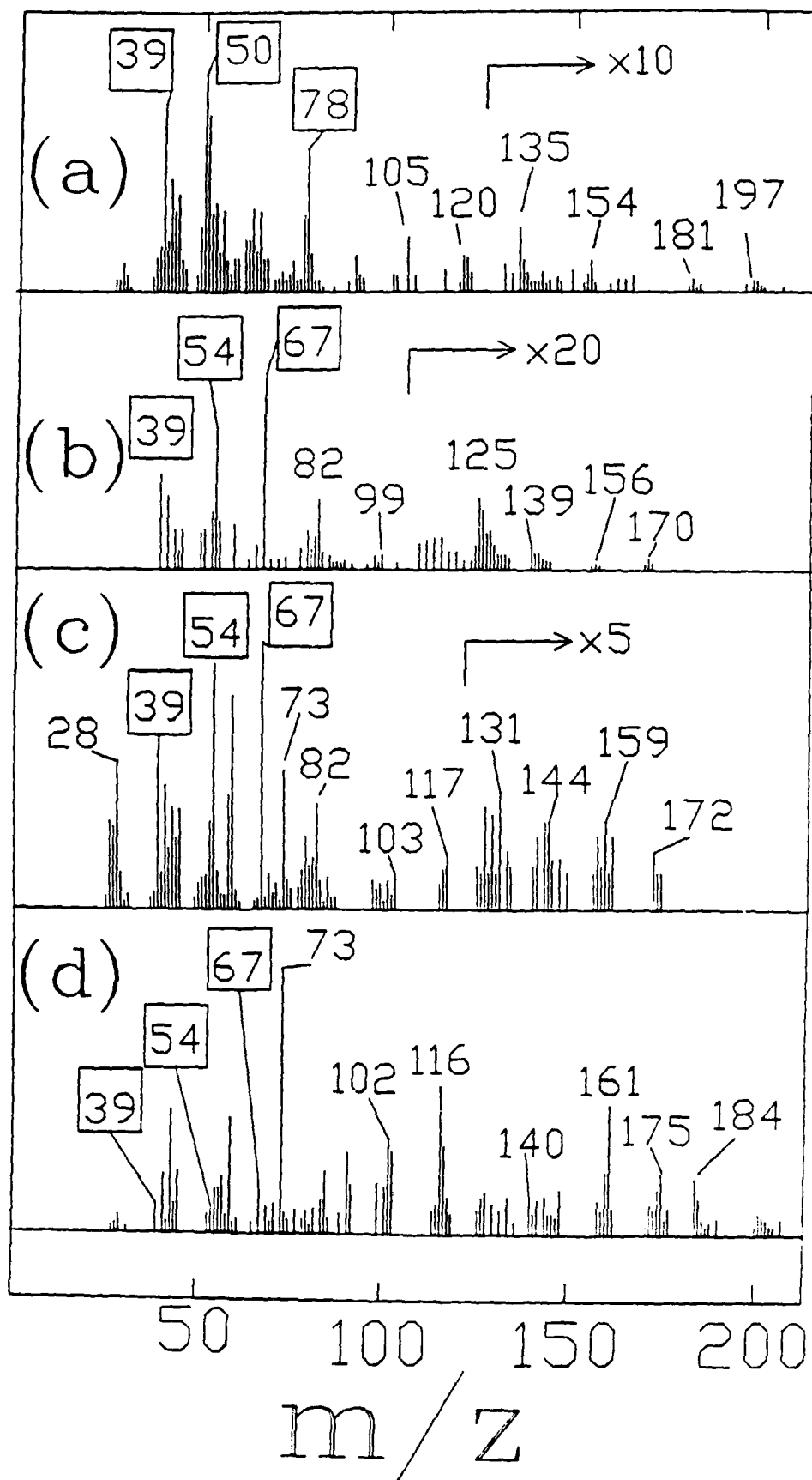
50

FIGURE 1

FIGURE 2

P−(Me$_2$Si)

(a)

Me$_2$Si$^+$

Me$_3$Si$^+$

(Me$_2$Si)$_2^+$

(Me$_2$Si)$_3^+$

(Me$_2$Si)$_4^+$

(Me$_2$Si)$_5^+$

I

×4

×1

100   200   300

m/z

(b)

43   59   73   85   101   116   131   143   159   173

I

×6

×1

50   100   150

m/z

FIGURE 3

(a) 42 43 59 73 86 127 145 172 ×10

(b) 41 56 73 85 101 114 129 143 ×10

(c) 42 55 70 87 101 115 129 142 171 ×15

(d) 41 56 69 84 99 115 129 143 170 199 ×5

m/z

50   100   150   200

I

FIGURE 5

I

—Si—CH$_2$—CH$_2$—   115   170   199

—Si—CD$_2$—CH$_2$—   117   172   203

—Si—CH$_2$—CD2—   118   172   203

—Si—*CH$_2$—CH$_2$—   116   171   201

m/z.

FIGURE 6

P-(Me$_2$Si)

I

345   385   425   465   505

λ(nm)

(a)

45 59

39   73 $\rightarrow$×5

        83
           99 113   143 157

I   (b) 59 73

39   115 $\rightarrow$×5

        101   129 143
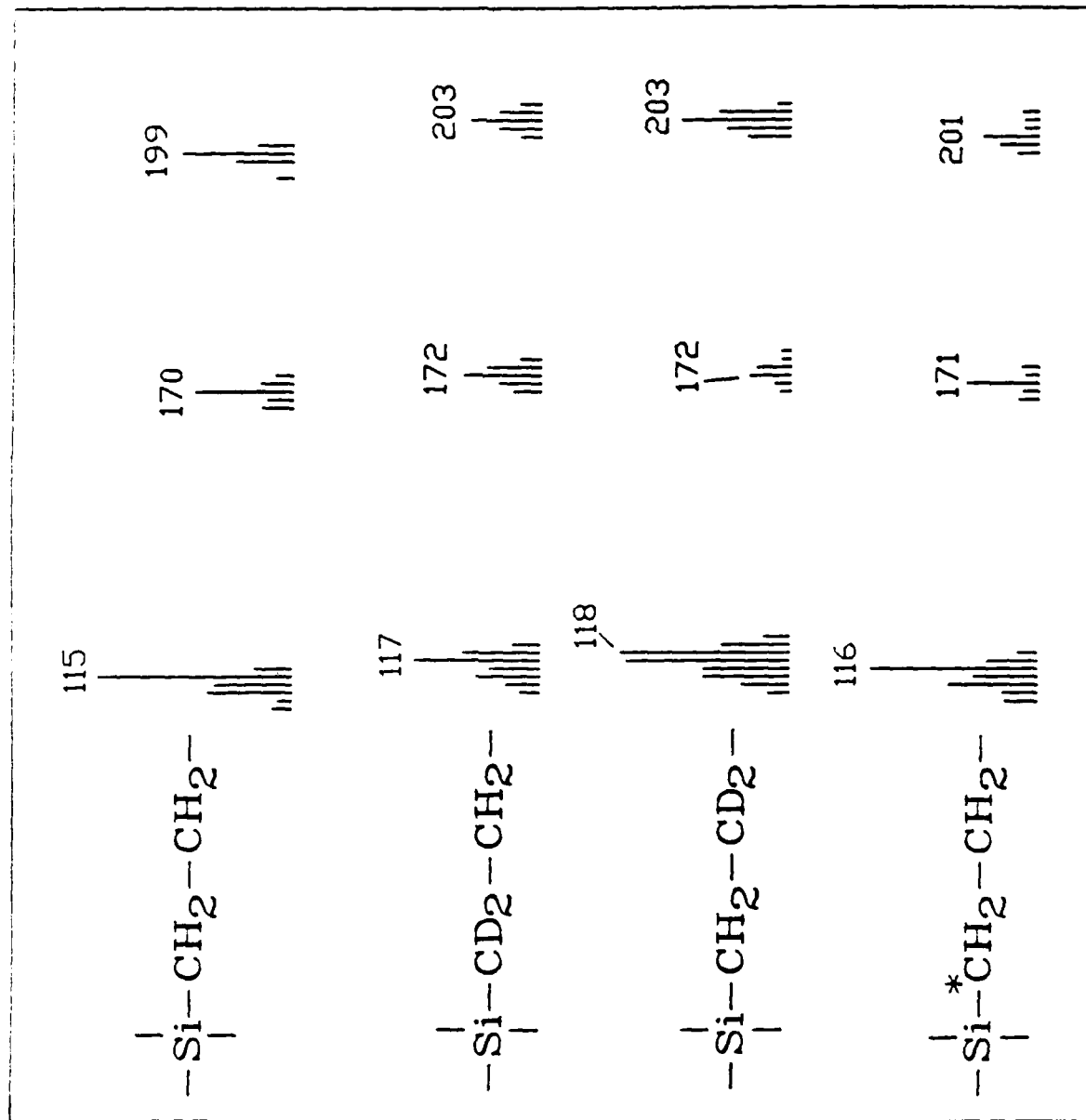   157
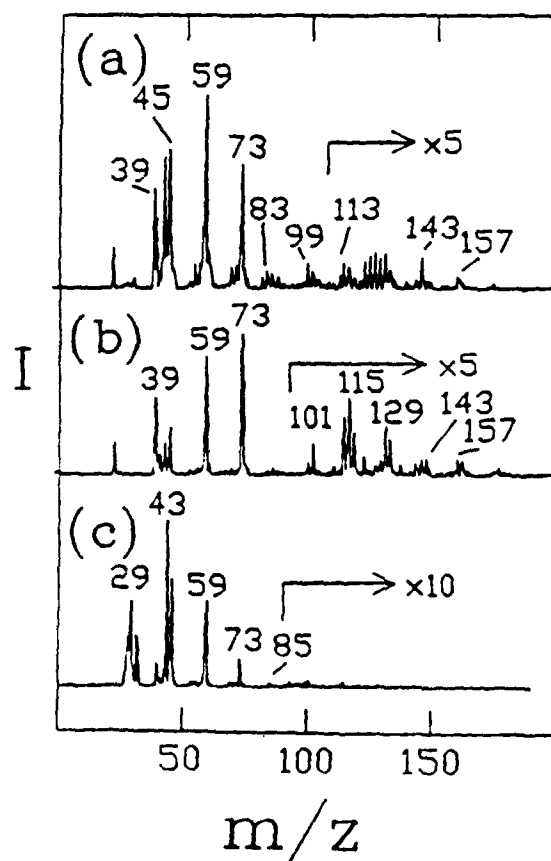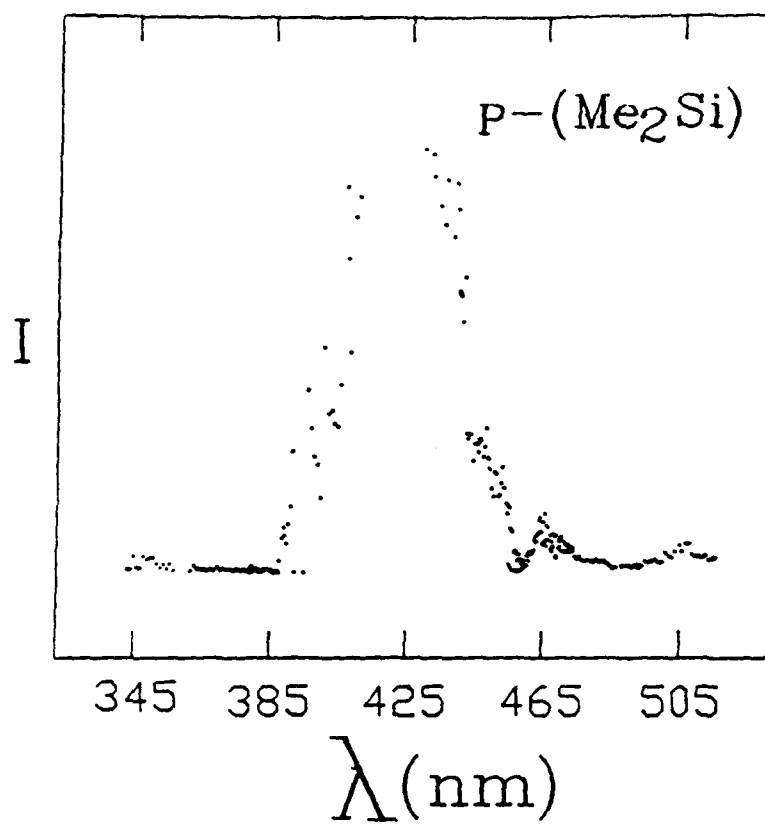
(c) 43

29   59

     73 85 $\rightarrow$×10

50   100   150

m/z

FIGURE 7

LASER DESORPTION MASS SPECTROMETRY OF POLYSILANES

Thomas F. Magnera*, V. Balaji and Josef Michl*

Center for Structure and Reactivity, Department of Chemistry,

The University of Texas at Austin, Austin, TX 78712-1167

R. D. Miller, and R. Sooriyakumaran

IBM Research Laboratories, Almaden Research Center, San Jose, CA
95120-6099

DETAILED DESCRIPTION OF THE LASER ABLATION MASS SPECTRA OF POLYSILANES

P-(Me$_2$Si) (Fig. 3). Ions much larger than monomeric Me$_2$Si$^{\bullet+}$ represent the bulk of the ions present.

Closed-shell ions. The complex sequence of closed-shell ions extends to masses near (Me$_2$Si)$_5$. The base peak at m/z = 59 corresponds to Me$_2$HSi$^+$. This and the other prominent peaks are of the type Me$_{2n-k+1}$H$_{k-2}$Si$_n^+$ and are assigned the structures of silicenium cations carrying hydrogen, methyl, and/or (partially or fully methylated) silyl substituents: R$_1$R$_2$R$_3$Si$^+$, R=H, Me, Me$_3$Si, etc.

For several of these ions, the structure assignment was confirmed by CID experiments (Table 1). Comparison with previous CID work was possible in the case of Me$_3$Si$^+$.[18]

The remainder of the ions are of the type Me$_{2n-k+1}$H$_{k-2}$Si$_n^+$.

1

n$\geq$2, and their structures must be unsaturated or cyclic. The requirement for the presence of two Si atoms, the results of CID experiments, and stability considerations suggest that these may be 1,3-disilaallyl cations carrying hydrogen, methyl, and/or partially or fully methylated silyl substituents: RR'Si=CH-Si$^+$R''R'''. The CID losses for several of these are listed in Table 1. Some precedent exists for such a structural assignment and for these dissociation processes, such as the elimination of CH_2=Si=CH_2.[14] However, cyclic structures can also be imagined, such as silicenium ions derived from 1,3-dis-ilabutane, with a methyl group or groups on the silicons.

Open-shell ions. The $Me_2Si^{\bullet +}$ ion is present at about a third of the intensity of Me_2HSi^+ and its structure could be $(Me-Si-Me)^{\bullet +}$ or $(CH_2$=SiHMe$)^{\bullet +}$. The next important open-shell ion is $Me_4Si_2^{\bullet +}$ at m/z=116, to which we assign the structure of the tetramethyldisilene radical cation $(Me_2Si$=$SiMe_2)^{\bullet +}$ since upon CID it loses a methyl group and produces daughter ions at m/z = 73 and 101. A metastable loss of $CH_3^{\bullet}$ from this ion has been reported.[20]

A third open-shell ion is at m/z=158, and a possible structure is $Me_2Si^{\bullet}$-Si(=CH_2)-Si$^+Me_2$. Low signal intensity prevented a measurement of a CID spectrum.

The open-shell ion $(Me_6Si_3)^{\bullet +}$ is quite weak and $(Me_8Si_4)^{\bullet +}$ is not observable, but $(Me_{10}Si_5)^{\bullet +}$ appears to be present, albeit weakly. It presumably has a cyclic structure with a five-membered ring of silicons.[16]

2

P-(Hx$_2$Si) and Its Isotopomers.   In a high sensitivity low-resolution spectrum local relative intensity maxima were found for ions near masses corresponding to (Hx$_2$Si)$_2^{\bullet+}$, Hx$_3$Si$_2^+$, Hx$_3$Si$^+$, Hx$_2$Si$^{\bullet+}$ and HxSi$^+$.   Peak widths were greater than 5 amu and for example (Hx$_2$Si)$_2^{\bullet+}$ was therefore not distinguishable from (Hx$_2$Si)$_2$H$^+$.   Starting with the dimer each local maximum was echoed at masses lower by 28 and 56 amu, corresponding to a loss of one and two molecules of ethylene, respectively.   In a high resolution spectrum the signal intensity was low at the higher masses.

Closed-shell ions.   A series of prominent peaks, including the base peak at m/z - 73, are of the type C$_n$H$_{2n+3}$Si$^+$ with n ≤ 12, and form the intense low-mass portion of the spectrum [Fig. 4]. These ions are most likely associated with singly, doubly, or triply alkylated silicenium cations such as H$_2$EtSi$^+$ or HMe$_2$Si$^+$ (m/z - 59), H$_2$PrSi$^+$, HMeEtSi$^+$ or Me$_3$Si$^+$ (m/z - 73), H$_2$BuSi$^+$, HMePrSi$^+$, etc., (m/z - 87), H$_2$PnSi$^+$, HMeBuSi$^+$, etc., (m/z - 101), H$_2$HxSi$^+$, HMePeSi$^+$, etc., (m/z - 115), HMeHxSi$^+$, HEtPnSi$^+$, etc., (m/z - 129) and HEtHxSi$^+$, MeEtPnSi$^+$, etc. (m/z - 143).

The isotopic intensity distribution in the ions C$_3$H$_9$Si$^+$ and C$_2$H$_7$Si$^+$ in the spectrum of P-(Hx$_2$Si)-α-^{13}C is instructive.   Both fit binomial distributions, [^{13}C$_0$]:[^{13}C$_1$]:[^{13}C$_2$][^{13}C$_3$] - (1-p)^3: 3(1-p^2)p:3(1-p)p^2:p^3, and [^{13}C$_0$]:[^{13}C$_1$]:[^{13}C$_2$] - (1-p)^2:2(1-p)p-p^2, with p - 0.35.   This probability is twice that expected if all carbon positions in the n-hexyl group were equally likely to be bonded to the silicon in the observed ion.   If the silicon always stayed attached to its α carbon, the C$_3$H$_9$Si$^+$ ion could never

3

contain three ^{13}C atoms. We conclude that the silicon shifts to other carbons, but not randomly. Since H_2PrSi^+, $HMeEtSi^+$, and possibly $i\text{-}PrH_2Si^+$ may be all contributing to the ion at $m/z =$ 73, and H_2EtSi^+ as well as HMe_2Si^+ may be contributing to the ion at $m/z =$ 59, we have not been able to carry the analysis further in an unambiguous fashion. The deuterium isotopic intensity distribution in these small ions and many others in the spectra of $P\text{-}(Hx_2Si)\text{-}\alpha\text{-}D$ and $P\text{-}(Hx_2Si)\text{-}\beta\text{-}D$ are difficult to unravel because of the mutual overlap of the isotopic patterns. There is ample evidence for very extensive scrambling, however.

The more tractable patterns are presented in Fig. 5 which features the quite intense peaks for the HHx_2Si^+ ion at $m/z =$ 199 and for the H_2HxSi^+ ion at $m/z =$ 115, smaller by C_6H_{12}. α-Substitution by ^{13}C changes the m/z values to 201 and 116, respectively, as expected for the loss of hexene with its α carbon. α-Disubstitution by ^2H changes them to 203 and 117, respectively, indicating that both $\alpha\text{-}^2H$ atoms are missing. On the other hand, β-disubstitution by ^2H produces 203 and not only 117 but also an equal amount of 118. Apparently, much of the time, a deuterium atom which was in a β position in the polymer is now located on the Si atom in the hexylsilyl cation. The overall isotopic pattern is compatible with a quite selective cleavage of the Si-C bond and transfer of a β hydrogen on the silicon, resulting in the formation of 1-hexene. It is not clear from the above whether the process occurs before electron impact ionization, or after ionization, or both. However, as we shall

4

see below, CID experiments on analogous ions obtained from p-(Pn_2Si) suggest strongly that at least in that case, the alkene loss occur both before and after ionization.

A second series of prominent peaks are of the type $C_nH_{2n+1}Si^+$ for $4 \leq n \leq 12$. This series is less intense except for the peaks at n=5 (m/z = 99), n = 6 (m/z = 113), and n = 12 (m/z = 197). A third, very weak series of the type $C_nH_{2n-1}Si^+$ is also observed. These series may be the unsaturated, cyclic or bicyclic analogs of the first. All three series have notably weak ions at masses one and three CH_2 units from the closed-shell pair at m/z = 197 and 199 corresponding to n = 5 and 7. Ions with these masses were also found in the mass spectrum of H_3HxSi.

Open-shell ions. Intense open-shell ions occur at m/z = 86, 114, 116, 128, 144, 170, 198 and 200. The ions at m/z = 198 and 200 are assigned to $Hx_2Si^{\bullet+}$ and $H_2Hx_2Si^{\bullet+}$ and those at m/z = 114 and 116 to $HHxSi^{\bullet+}$ and $H_3HxSi^{\bullet+}$. The ion at m/z = 86, presumably either $PrHSi-CH_2^{\bullet+}$ or $EtCH-SiHMe^{\bullet+}$, also appears as a prominent ion in the mass spectrum of H_3HxSi. The ions at m/z = 170, 144, 128 and 114 are associated with formal losses of ethylene, butene (or two molecules of ethylene), pentene, and hexene, respectively, from $Hx_2Si^{\bullet+}$. The ion m/z = 86 can be associated with a loss of ethylene from $HHxSi^{\bullet+}$.

Once again, isotopic shift patterns are instructive only for a few ions. Figure 5 displays the relatively intense open-shell ion peaks at m/z = 170 and m/z = 198 ($Hx_2Si^{\bullet+}$), related by the loss of C_2H_4. Upon introduction of α-^{13}C atoms, the peaks shift

5

to m/z - 171 and m/z - 200, showing clearly the loss of one α
carbon. Upon dideuteration in either the α or the β position,
they shift primarily to m/z - 172 and m/z - 202, but peaks at m/z
- 171 and 173 are also significant. These results demonstrate
that the ethylene unit missing in the m/z - 170 ion consists of
the α and β carbons and their hydrogens, with a moderate amount
of scrambling. This suggests the HxBuSi$^{\bullet+}$ structure for this ion.
Once again, we cannot tell whether the α,β-ethylene loss occurs
before or after electron impact ionization, or both.

Ions due to 1-hexene. The spectrum of P-(Hx$_2$Si) contains
intense peaks at m/z - 84, 69, 56, 55, 42, 41 and 40, all of
which have relative abundances that match closely the standard
fragmentation pattern of 1-hexene or cyclohexane. Deuteration in
the α and β positions leads to molecular ion shifts by +2 and +1,
respectively, and introduction of ^{13}C in the α position to a
shift by +1, allowing the clear assignment of the spectrum to 1-
hexene formed by the cleavage of the Si-C bond and loss of a β
hydrogen. There is evidence of a very small amount of scrambling
in the labeled positions, and the isotopic behavior parallels
clearly that described above for closed-shell silicon-containing
ions.

A simple explanation of the presence of 1-hexene would be
that it is directly produced in the ablation process. However,
it is also possible that the hexene is produced in a post-ioniza-
tion process. In order to distinguish between these pos-
sibilities, two experiments were done. The EI-MS of n-hexylsilan

6

was obtained. A fragment ion corresponding in mass to 1-hexene was observed but not the complete set of 1-hexene peaks. The second experiment involved trapping of the ablated material at a low temperature and its analysis by GC-MS. 1-Hexene was found unequivocally. The yields were small, presumably due to the inefficiency of the trapping method and not necessarily due to a low absolute yield.

We conclude that 1-hexene is formed in the ablation process, and it is most economical to assume that this is the same loss that has been deduced from consideration of the closed-shell ions containing silicon (Fig. 5). If this is correct, the β-hydrogen lost from the hexyl chain ends up on the nearby silicon. The absence of significant isotopic scrambling in the 1-hexene product suggests that much of the scrambling observed in the closed-shell and open-shell silicon-containing cations results from events not involving the hexyl substituent and quite possibly subsequent to the loss of hexene.

The mass spectra also contain weak unassigned peaks at m/z = 67 and m/z = 70 which may be indications of the presence of cyclohexene and 1-pentene, respectively. Positive identification is prevented by the overlap with the much more intense 1-hexene ion-fragmentation pattern.

P-(Pn$_2$Si). *Closed-shell ions*. The alkyl chain fragmentation series, $C_nH_{2n+3}Si^+$, previously described for P-(Hx$_2$Si), is again the major contributor to the low-mass portion of the spectrum (Fig. 4). CID of the peak at m/z = 73 generates daughter ions at

$m/z = 45$ and 43 at a collision energy of 5 eV(lab) with a branching ratio greater than 9. Since CID done on the Me_3Si^+ ion generated from EI of tetramethylsilane yields only the $m/z = 45$ ion[18], at least some of the intensity at $m/z = 73$ clearly corresponds to the isomeric forms such as $HEtMeSi^+$ or H_2PrSi^+.

The $C_nH_{2n+3}Si^+$ series is accompanied by a $C_nH_{2n+1}Si^+$ ($n > 3$) series of comparable intensity. In both series, n runs up to 10 and the peaks at $n = 9$ have only weak intensity. Strong intensities are found at $n = 5$ and 10 and correspond to the ions $m/z = 99$ and 101 ($PnSi^+$ and H_2PnSi^+) and $m/z = 169$ and 171 [$(Pn_2Si - H)^+$ and HPn_2Si^+]. The series $C_nH_{2n-1}Si^+$ is also present and the ion at $m/z = 97$, $(PnSi-2H)^+$, is anomalously intense.

It is of interest to note that CID on the HPn_2Si^+ ion produces a loss of C_4H_8 to yield $m/z = 115$, presumably $HMePnSi^+$, and a loss of C_5H_{10} to yield $m/z = 101$, presumably H_2PnSi^+, with comparable intensities. On the other hand, in the EI mass spectrum of the ablated material, the $m/z = 101$ peak is much stronger than the $m/z = 115$ peak. This suggests that some of the pentene loss occurs already before the ionization event, while some clearly occurs afterward.

Open-shell ions. Open-shell ions are found at $m/z = 72$, 86, 100, 114, 128, 142 and 170, with $m/z = 100$ ($HPnSi^{\bullet+}$), 142 and 170 ($Pn_2Si^{\bullet+}$) being particularly intense. The ions at $m/z = 142$ and 114 correspond to losses of one and two ethylene molecules from $Pn_2Si^{\bullet+}$, respectively. The ion at $m/z = 100$ may result from a similar loss of pentene.

8

Ions due to 1-pentene. The most intense ions in the low-mass portion of the spectrum, m/z = 70, 55, 42, 41 and 39, closely match the MS of pentene and are assigned in analogy with the P-(Hx$_2$Si) results.

P-(Bu$_2$Si). *Closed-shell ions.* Again the fragmented alkyl chain series ions $C_nH_{2n+3}Si^+$, $C_nH_{2n+1}Si^+$ and $C_nH_{2n-1}Si^+$ are observed with strong peaks at n = 4, 5 and 6 (Fig. 4). The dealkylated monomers and the monomer of these series are locally intense.

Open-shell ions. Open-shell ions were found at m/z = 72, 86 (HBuSi$^{\bullet+}$), 100 (MeBuSi$^{\bullet+}$), 114 (EtBuSi$^{\bullet+}$), 128 (PrBuSi$^{\bullet+}$), and 142 (Bu$_2$Si$^{\bullet+}$). The peak at m/z = 114, corresponding to a loss of ethylene from Bu$_2$Si$^{\bullet+}$, is prominent.

Ions due to 1-butene. The presence of 1-butene is inferred from the presence of strong peaks at m/z = 56, 55, 41 and 39 and the behavior of P-(Hx$_2$Si) and P-(Pn$_2$Si).

P-(MePrSi). A low-resolution spectrum has discernible local maxima occurring near (MePrSi)$_3$$^{\bullet+}$, [(MePrSi)$_3$ - C$_2$H$_4$]$^{\bullet+}$, Me$_3$Pr$_2$Si$_3$$^+$, (MePrSi)$_2$$^{\bullet+}$, [(MePrSi)$_2$ - C$_2$H$_4$]$^{\bullet+}$, Me$_2$PrSi$_2$$^+$, MePrSi$^{\bullet+}$, [MePrSi - C$_2H_4$]$^{\bullet+}$, and MeSiH$^{\bullet+}$. The peak widths were approximately 5 amu. Very weak signals were detected for masses greater than the trimer.

Closed-shell ions. The base peak for the spectrum (Fig. 4) of P-(MePrSi) is HMe$_2$Si$^+$ (m/z=59). The series $C_nH_{2n+3}Si^+$ is the major contributor to the low-mass portion of the spectrum. At higher masses, this series is accompanied by the two additional

series, $C_nH_{2n+1}Si^+$ and $C_nH_{2n-1}Si^+$.

Open-shell ions. There are three very strong open-shell at m/z = 58 ($Me_2Si^{\bullet+}$), m/z = 86 ($MePrSi^{\bullet+}$) and m/z = 172. Tl last one is assigned the disilene structure $[MePrSi=SiMePr]^{\bullet\cdot}$ The P-(MePrSi) spectrum is particularly rich in other open-sl ions which correspond to the radical cations of disilenes ca various numbers of H, Me, and Pr substituents (m/z = 102, 11(130, 144, and 158).

Ions due to propene. There is an intense peak at m/z = and a second peak at m/z = 41. These are associated with C_3 and $C_3H_5^+$, respectively.

P-(MeChSi). *Closed-shell ions.* The series $C_nH_{2n+3}Si^+$ i present (Fig. 6) but is less prominent than usual, and exten only to n = 4. There are considerably fewer closed-shell io there is no discernible 14 amu degradation pattern character of the linear alkyls, and only sporadically occurring member the series $C_nH_{2n+1}Si^+$ and $C_nH_{2n-1}Si^+$. The protonated monome $HMeChSi^+$ at m/z = 127 is much weaker than usual. The ion co responding to $HC^+=SiHCh$ or an isomer however has normal inte relative to the monomer. For masses greater than the monome only two significant groups of ions were observed, one at o(masses between m/z = 189 and 145, and a pair at m/z = 169 a 171. The last ion corresponds to the structure $H_2MeSi-Si^+M$ one of its isomers. There are also ions at odd masses from through 115 which at least formally correspond to [ChSi - 2 $ChSi^+$, H_2ChSi^+ and H_2HxSi^+, respectively.

These results can be compared with the EI mass spectrum of HMe_2ChSi, which has peaks at m/z - 97, 99, and 127.

Open-shell ions. The monomer ion $MeChSi^{•+}$, m/z - 126, is most intense silicon-containing open-shell ion in the spectrum. It is accompanied by a series of ions at m/z - 128, 130, 132. Other open-shell ions larger than the monomer occur at m/z - 17($(HMeSi=SiMeCh^{•+})$ and a group at m/z - 140, 142 and 144.

Ions due to cyclohexene. The most intense ions in the low mass portion of the spectrum, m/z - 82, 67, 54, 41 and 39, closely match the MS of cyclohexene. This assignment was confirmed by GC-MS of trapped material and by comparison with the EI-MS spectrum of HMe_2ChSi, which also has a strong signal at m/z - 82 but much weaker signals at 67, 54, 41, etc.

p-(MePhSi). *Closed-shell ions.* This spectrum (Fig. 6) is very different from the spectra of the alkylpolysilanes. There are very few silicon-containing closed-shell ions, and the seri $C_nH_{2n+3}Si^+$ is absent, even for small n. Those observed are m/z - 43 ($MeSi^+$ or an isomer), 121 ($HMePhSi^+$), 135 (Me_2PhSi^+), 197 ($MePh_2Si^+$). The ion corresponding to $(MePhSi - H)^+$ (m/z - 119) is at least five times weaker than $HMePhSi^+$.

Open-shell ions. The ion of the monomer, $MePhSi^{•+}$, is present at m/z - 120 but is less intense than the peak at m/z - 105, isomeric with $PhSi^+$. No other open-shell Si-contain ions could be assigned.

Ions due to benzene and toluene. The low-mass spectrum consisted almost entirely of peaks from the overlap of the mass

11

spectra of benzene and toluene. GC-MS trapping established th

both benzene and toluene are generated before ionization.

P-(Me$_2$SiMeChSi). The spectrum of this 1:1 copolymer (Fig

was similar to a superposition of the spectra of the homopolyr

P-(Me$_2$Si) and P-(MeChSi), with the former significantly more

intense, particularly in the high mass region where ions conta

ing two or three silicons are much more likely to contain meth

groups than cyclohexyl groups. This may simply be a reflectio

of the fact that many of the cyclohexyl groups have been lost

the form of cyclohexene.

Closed-shell ions. The series Me$_{2n-k+1}$H$_{k-2}$Si$_n^+$, which wa

also observed for P-(Me$_2$Si), is evident but weak for ions with

> 3. Notably weak are the ions assigned to HMeChSi$^+$ (m/z = 1:

and (MeChSi - H)$^+$.

Open-shell ions. The only open-shell ions with signific

intensity are Me$_2$Si$^{\bullet+}$ (m/z = 58) and Me$_2$Si=SiMe$_2^{\bullet+}$ (m/z = 116)

Ions due to cyclohexene. The predominant peaks are m/z

82, 67, 54, 41, and 39, and these are assigned to cyclohexene

Table 1

$P-(Me_2Si)$ - Closed-shell ions

Series	m/z	Losses	Proposed Structure
$Me_{2n-k+1}H_kSi_n^+$	73	C_2H_6; C_2H_4	Me_3Si^+
	117	$H_2Si=CH_2$	Me_3Si-Si^+HMe
	131	Me_2Si	$Me_3Si-Si^+Me_2$
$Me_{2n-k+1}H_{k-2}Si_n^+$	101	$Si=CH_2$	$Me_2Si=CH-Si^+H_2$
	115	$H_2Si=CH_2$	$HMeSi=CH-Si^+Me_2$
	129	$H_2C=Si=CH_2$; C_2H_4; $MeHC=Si$; $Si=CMe_2$	$Me_2Si=CH-Si^+Me_2$
$Me_{2n-k+1}H_{k-4}Si_n^+$	85	$HSiCH$; CH_4	$CH_3-SiH=C=SiH$
	99	none observed	

13